ABSTRACT

Title of Thesis: EXPLORING THE TEMPERATURE AND HYDROLOGIC RESPONSE OF TROPICAL OCEANS TO VOLCANIC ERUPTIONS OVER THE LAST 400 YEARS USING CORAL GEOCHEMISTRY

Zoraida Paola Pérez Delgado,
Master of Science, 2020

Thesis Directed By: Dr. Kelly Halimeda Kilbourne,
Marine-Estuarine and Environmental Science

Volcanic eruptions perturb the Earth's climate system. Open questions remain about the response of the hydrologic cycle and internal variability. Coral skeletal strontium to calcium ratios (Sr/Ca) and oxygen isotopic ratios ($\delta^{18}O$) record temperature and seawater oxygen isotopic signatures in the oceans, thus climatic perturbations from eruptions may be recorded in the coral skeletal chemistry. I quantify the temperature and hydrologic response of the tropical climate system to eruptions since 1640 CE based on coral geochemical records. Data from all basins except the central and eastern Pacific show cooling and increases in seawater $\delta^{18}O$ within the first three years of an eruption. Statistical significance of identified signals was tested by comparing against non-eruption sections from the records. Analyses with paired Sr/Ca and $\delta^{18}O$ illustrate that the number of observations still limits detection of small signals provided by the eruptions.

EXPLORING THE TEMPERATURE AND HYDROLOGIC RESPONSE OF TROPICAL OCEANS TO VOLCANIC ERUPTIONS OVER THE LAST 400 YEARS USING CORAL GEOCHEMISTRY

by

Zoraida Paola Pérez Delgado

Thesis submitted to the Faculty of the Graduate School of the
University of Maryland, College Park, in partial fulfillment
of the requirements for the degree of
Master of Science
2020

Advisory Committee:

Associate Research Professor Dr. Hali Kilbourne, UMCES CBL, Chair
Professor Dr. Michael Evans, UMD College Park
Assistant Research Professor Dr. Vyacheslav Lyubchich, UMCES CBL

Dedication

I dedicate this to my loving family for always believing in me, even when I did not.

Acknowledgements

I want to thank my mother, Zoraida Delgado Hernández, my father, Jorge A. Pérez Rivera, and my friends and family for all of the help and support that they brought me these years. I would not have been able to do this without them. Muchas gracias.

Table of Contents

List of Tables

List of Figures

Chapter 1: Introduction

1.1 Volcanic Eruptions and the Earth's Climate

Stratospheric aerosol forcing from volcanic eruptions provide a mechanism to test Earth system model responses to radiative forcing (Crowley & Unterman, 2013), particularly changes in Earth's energy balance driven by internal feedbacks and external forcing (Fischer *et al*., 2007). Strong volcanic eruptions create a testable perturbation by altering the Earth's albedo, cooling Earth's temperature, and eliciting changes in precipitation patterns (Man *et al.,* 2014; Joseph and Zeng, 2011; Mann *et al.,* 2015; Winter *et al.,* 2015; Gao *et al.,* 2017; Iles *et al*., 2013; Gao *et al.,* 2017; Gillett *et al.,* 2004).

Eruptions inject ash, halogens, dust and aerosol particles into the atmosphere (Robock, 2000; LeGrande *et al.,* 2016). The sulfur dioxide (SO_2) gas emitted in the volcanic eruption is oxidized to sulfuric acid that ultimately creates a fine aerosol cloud (Zanchettin *et al.,* 2013; Iles *et al.,* 2013; Man *et al.,* 2014; Mann *et al*., 2015; Robock, 2014). If the ash and aerosol particles are injected into the lower stratosphere, they will become globally distributed, reflect incoming solar radiation and perturb Earth's radiative balance. For example, the 1815 Mt. Tambora eruption reduced global incoming radiation by an estimated -17.20 W/m^{-2} (Zanchettin *et al*., 2013). Once in the stratosphere, the particle size dictates the residence time of the aerosols (Lacis *et al.,* 1992; Crowley and Unterman, 2013). Larger particles fall out more quickly whereas smaller particles take longer to fall.

Stratospheric injection of volcanic aerosols leads to many changes, not just environmental but also societal and economic (Robock, 2000; Guillet *et al*., 2017; Gao *et*

al., 2017; Gillett *et al*., 2004). For example, the 1257 Samalas eruption has been associated with crop failure and spatially heterogeneous cooling periods across the Northern hemisphere (Guillet *et al.,* 2017). Similarly, the 1815 Mt. Tambora eruption led to crop failures across the Northern hemisphere and produced the infamous "Year Without Summer" the following year (Gao *et al*., 2017).

When an eruption of sufficient magnitude occurs in the tropics, the aerosol cloud will move poleward with time resulting in changes to the global climate system (Robock, 2000; Iles and Hegerl, 2014) (Figure 1). The aerosol cloud alters Earth's albedo, effecting the global radiative energy balance (Man *et al.,* 2014; LeGrande *et al.,* 2016) and causing cooling periods in global temperature (Bradley, 1988; Robock, 2000; Iles and Hegerl, 2014; Sigl *et al.,* 2015; Zanchettin *et al.,* 2013). The cooling periods themselves vary with the intensity of the eruptions and occur because incoming solar shortwave radiation is reflected into space, thus cooling the planet by decreasing solar heating (Man *et al.,* 2014; Iles *et al.,* 2013). The exact duration of such periods depends on the specifics of any given eruption, but some studies have found that it could last 1-3 years (Fischer *et al.,* 2007; Stenchikov *et al.,* 2009). Existing background climate conditions and the season of the eruption could also affect the persistence of the cooling (Fischer *et al.,* 2007).

The spatial extent and climatic impact of a volcanic aerosol cloud on the Earth's climate depends on many factors such as cloud movements, seasonality (Fischer *et al.,* 2007; Stevenson *et al.,* 2017), particle size (Mann *et al.,* 2015), latitude and strength of the eruption, and the climatic background conditions that were present when the eruption took place (D'Arrigo *et al.,* 2013; Man *et al*., 2014; Stevenson *et al.,* 2017). Since this research will focus on the last 400 years, it is important to mention that some of the large volcanic

eruptions over that period have coincided with solar insolation minima (Shindell *et al*., 2001; Abram *et al.,* 2016; Wang *et al*., 2017) which makes it difficult to distinguish which forcing (solar or volcanic) had a more significant impact on the climate system based on observational data alone.

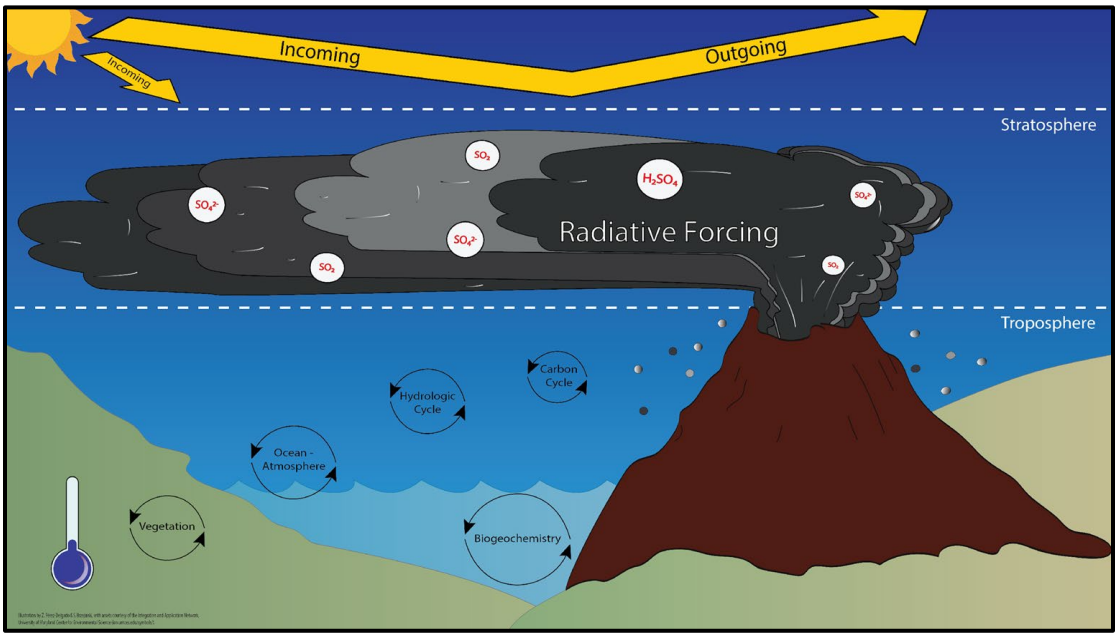

Figure 1. Effects of a large-scale stratospheric volcanic eruption on the climate system. The illustration was made with assets courtesy of the Integration and Application Network, University of Maryland Center for Environmental Science (ian.umces.edu/symbols/).

1.2 Influence of volcanic eruptions on climate patterns

Apart from altering the global temperature, volcanic eruptions have been tied to influencing atmospheric and oceanic circulation patterns (Mignot *et al.,* 2011), the El Niño-Southern Oscillation (ENSO) (Iles and Hegerl, 2014), Atlantic Multidecadal Variability (AMV) (Wang *et al.,* 2017), the North Atlantic Oscillation (NAO) (Fischer *et al*., 2007) and the Atlantic meridional overturning circulation (AMOC) (Stenchikov *et al.,* 2009; Pausata *et al.,* 2015). Volcanic forcing has also been known to affect the intensity and/or latitude of the Intertropical Convergence Zone (ITCZ) (Blake *et al.,* 2017; Pausata *et al.,* 2015; Stevenson *et al.,* 2017; Lechleitner *et al*., 2017). An analysis of multiple state of the

art climate models indicated that the cooling of a particular hemisphere by a volcanic eruption shifts the ITCZ away from the hemisphere of eruption instead of its normal seasonal pattern of being closer to the summer hemisphere (Iles and Hegerl, 2014).

Although volcanic eruptions have been tied to influencing these patterns of variability, the focus of many studies has been on assessing the Earth systems' responses to these events by doing model-to-model and model-to-satellite data comparisons (Iles *et al.,* 2013; Zanchettin *et al.,* 2013) with a particular focus on temperature changes and potential uses for geoengineering (Paik and Min, 2018). Modern multi-model and observational climate studies have started to focus on hydroclimate variability after an eruption by looking at the differences in terms of spatial precipitation patterns (Iles *et al.,* 2013; Joseph and Zeng, 2011; Wegmann *et al*., 2014; Paik and Min, 2018). Chen *et al.,* (2020) performed three sensitivity experiments, using the Community Earth System Model, to test how the magnitude and timing of a volcanic eruption could lead to various drought conditions (notably different lengths and intensity). These studies have found an overall reduction in global mean precipitation as a result of the decrease in temperature following strong eruptions over the last millennium (Iles *et al.,* 2013; Joseph and Zeng, 2011).

Open questions remain regarding the immediate effects of volcanic eruptions on the climate system such as the impact of volcanoes on decadal-scale variability (Crowley *et al.,* 1997, Otto-Bliesner *et al*., 2016), the role of volcanic eruptions on ocean heat content and uptake (Mignot *et al.,* 2011; Crowley and Unterman, 2013; Stenchikov *et al.,* 2009) and if strong stratospheric eruptions can trigger an ENSO event (Stenchikov *et al*., 2009; Iles and Hegerl 2014). Some of the latest modeling projects are trying to gain a better

understanding of the climate's response following an eruption (Timmreck, 2012; Zanchettin *et al.,* 2016; Marshall *et al.,* 2018; DallaSanta *et al.,* 2019). One of the ways this is being done is by comparing output from model simulations to paleoclimate reconstructions and observational datasets. Unfortunately, the model output does not always match the proxy reconstructions, resulting in an over or underestimation of the eruption's magnitude and temperature and precipitation changes from the simulations (Iles *et al*., 2013; Zanchettin *et al*., 2015; Paik and Min, 2018). Additional research needs to be done to fully understand the mechanistic connection between these large-scale eruptions and the climate system (Schmidt, 2010), as well as refining both paleoclimate reconstructions and model simulations to narrow the discrepancies that exist between the simulations and the reconstructions (Mann *et al.,* 2012; Sigl *et al*., 2015).

1.3 Understanding the Hydrologic and Temperature Response to Eruptions

Understanding past and future climate conditions requires accurate simulations using state-of-the-art Earth system models. However, climate models are validated against a limited number of historic volcanic eruptions for which a large number of instrumental observations are available for comparison. Paleoclimate proxies provide us with climate information about eruptions before the instrumental record, permitting model validation on a broader set of volcanic eruptions.

Working groups from the Past and Global Changes (PAGES) network, as well as some Model Intercomparison Projects (MIP), such as the MIP on the climatic response to volcanic forcing (VolMIP), have expressed an interest in improving the scientific communities understanding of how volcanic eruptions influence the hydrological cycle (PAGES Hydro2k Consortium, 2017; Zhou *et al.,* 2016; Zanchettin *et al.,* 2016). To do

this, a few working groups in the paleo community are creating new databases from proxy reconstructions to facilitate the interpretations of hydroclimate signals (PAGES Hydro2k Consortium, 2017), while some climate modeling projects are testing their response to volcanic eruptions in an attempt to reduce model uncertainty (PAGES Hydro2k Consortium, 2017; Zhou *et al.,* 2016; Zanchettin *et al.,* 2016).

Although research has been done on volcanic events using paleoclimate proxies, most of it focuses on terrestrial temperature changes after an eruption by using speleothems, ice cores, and tree rings (D'Arrigo *et al.,* 2008 D'Arrigo *et al.,* 2013; Man *et al.,* 2014). Generally, these studies find a temperature decrease after an eruption, with some temperature and precipitation discrepancies in climate models. Models are imperfect and it is a challenge to accurately capture the coupled ocean-atmosphere processes involved in a robust stratospheric eruption, such as volcanic radiative forcing, subgrid-scale physics, aerosol particle size and distribution, and the relationship between regional/local environmental conditions and atmospheric/oceanic circulation (Timmreck, 2012; Mann *et al.,* 2012; Sigl *et al.,* 2015; Zanchettin *et al.,* 2015). This existing research gives an insight into the immediate climate response to eruptions, especially in terrestrial environments. However, more research is needed to understand the oceanic response to these eruptions, as well as the volcanic eruption's connections to natural ocean-connected phenomena such as AMV and ENSO events.

AMV, the primary mode of multi-decadal climate variability in the Atlantic Ocean sector, has long been an area of interest in both the paleoclimate and modeling communities. Modeling studies focusing on the Last Millennium and the Little Ice Age have shown periods of decadal-scale variability being tied to volcanic forcing (Otto-

Bliesner *et al.,* 2016), while paleoclimate research carried out with terrestrial proxies over the Northern Hemisphere have shown that strong volcanic eruptions may trigger cool phases of AMV (Wang *et al.,* 2017).

The climate community is also interested in exploring the potential linkage of volcanic eruptions to ENSO, an internal mode of variability in the climate system that could be excited by a volcanic event (Adam *et al.,* 2003; Stenchikov *et al*., 2009; Otto-Bliesner *et al.,* 2016). ENSO is a natural phenomenon with altering cold (La Niña) and warm (El Niño) phases (Neelin *et al.,* 1998). It occurs every two to seven years in the tropical Pacific Ocean and leads to global changes in SST, SSS and precipitation patterns (Robock 2000, Gillet *et al.,* 2004; McPhaden *et al.,* 2006; Gu and Adler, 2010). In a model ensemble study, Stevenson *et al.,* (2016) showed that ENSO events respond to large stratospheric eruptions in the tropics and extra-tropical regions. Their experiments demonstrated that the ENSO response (warm or cold phase) depends on the hemisphere where the volcanic eruption occurred. This type of reaction is potentially tied to the shifting of the ITCZ to the warmest hemisphere after a strong temperature changing eruption has taken place (Stevenson *et al.,* 2016).

Lehner *et al.,* (2016) showed that sampling biases within models could explain how models tend to overestimate temperature changes after a volcanic eruption. McGraw *et al.,* (2016) looked at the disagreement between observational studies and models on the sign of the tropospheric temperature response at the time of the eruption, finding the discrepancy to be potentially due to the internal variability of the climate system and the state/phase of ENSO at the time of the eruption. Discrepancies between modeling and observational studies exist in terms of temperature overestimation by models occurring in

the year of and after the eruption, as well as a tendency for models to apparently overestimate the magnitude of temperature decrease after an eruption occurs (McGregor and Timmerman, 2011; Stevenson *et al.,* 2016; Lehner *et al.,* 2016). Despite our understanding of the basic behavior of ENSO (Zebiak and Cane, 1987), discrepancies exist in the responses of ENSO to volcanic eruptions between different investigative approaches; modeling, modern observations and paleoclimate observations (Stevenson *et al.,* 2016; Otto-Bliesner, 2016). Ultimately, more research is needed to improve our understanding of ENSO variability and how it relates to radiative forcing from volcanic eruptions.

1.4 Brief Description of this Study

This research aims to use tropical coral geochemical records of climate from the past 400 years to improve our understanding of the hydroclimate and temperature response in the global tropical oceans after a strong volcanic eruption occurs. I focus on the global tropics since perturbations in the tropics often have global repercussions because excess solar energy in the tropics fundamentally drives the global ocean and atmosphere circulation patterns that make up our climate system (Hastenrath, 1991). The use of coral geochemical records provides centuries-long time series with no seasonal bias, because the species used are tropical taxa that grow year-round. Tropical corals are also fast growing, providing monthly to annual resolution, and their aragonite skeletons have annual density bands with the option of radiometric dating that enables exceptional age control from a marine paleoclimate archive.

1.5 Coral records as proxies for temperature and rainfall

Corals are affected by the temperature and chemistry of the surrounding seawater (Tierney *et al.,* 2015). Their skeletons can record a variety of environmental variables in their chemical make-up, including variations in ocean temperature and seawater oxygen isotope composition, which in turn can enable inference about past hydrologic conditions (Jones *et al.,* 2009). Coral geochemical records of strontium to calcium ratios (Sr/Ca) are primarily a function of temperature, while the oxygen isotopic ratios ($\delta^{18}O$) primarily reflect a combined signal of temperature and the $\delta^{18}O$ of seawater ($\delta^{18}O_{sw}$). Composition of $\delta^{18}O_{sw}$ depends primarily on the hydrologic cycle in the modern ocean, specifically the regional balance of evaporation and precipitation, which is also a driver of open-ocean sea surface salinity (SSS, Epstein *et al.,* 1953; Fairbanks *et al.,* 1997; Kilbourne *et al.,* 2004; Cahyarini *et al*., 2008; Bolton *et al.,* 2014). Thus, these coral geochemical records work as natural temperature and salinity loggers, providing indirect measurements of temperature and precipitation in a location over the time of coral growth.

Paired Sr/Ca and $\delta^{18}O$ coral records, can be used to calculate the $\delta^{18}O_{sw}$ which, as mentioned above, can be a signal of seawater salinity (Fairbanks *et al.,* 1997). This is done by removing the Sr/Ca temperature signal from the $\delta^{18}O$ to obtain a residual $\delta^{18}O$ signal attributed to the $\delta^{18}O_{sw.}$ The resulting $\delta^{18}O_{sw}$ deciphered from the coral record provides information about hydroclimate variability (Bolton *et al.,* 2014).

Although coral records are great temperature loggers, some uncertainties associated with them cannot be ignored. Uncertainty in coral records can come from sub-sampling, diagenetic alteration, calibration and analytical precision, and depth and age (Sowa *et al.,* 2013; Comboul *et al.,* 2014; Flannery *et al.,* 2017; Sivaguru *et al.,* 2019).

When extracting a core, the topmost part of the core will be the most recent year, and the previous bands will be representative of the earlier years as one starts counting backward till reaching the end of the core. Aligning the count across core breaks can lead to some sampling or human errors. Diagenetic processes can influence the isotopic and elemental content of the corals, influencing the derived temperatures and making reliable temperature reconstructions impossible (Takada *et al.,* 2017). Additionally, uncertainties in their layer-counted chronologies or age models are expected coral records. One possible way to decrease the age uncertainty associated with the records, assuming all other sources of uncertainty have been accounted for, is to do essentially event stratigraphy and identify specific climatic events or markers in multiple records (DeLong *et al.*, 2013; Comboul *et al.,* 2014).

1.6 Research Questions

To work towards an assessment of the tropical hydrologic and temperature response to strong volcanic eruptions, I conducted an analysis of existing coral Sr/Ca and $\delta^{18}O$ records. The goal of this research was to explore whether the climate response to volcanic events is recorded in coral Sr/Ca and $\delta^{18}O$ above the background climate fluctuations.

To achieve the goal, I attempted to answer the following three questions:

1. How sensitive are coral geochemical records to capturing individual volcanic event signals? Can a climate signal be detected from corals that grew during the relatively small 1991 Mt. Pinatubo eruption?
2. Can we detect the climate impact of a much bigger eruption, with a more limited coral network, for instance, the Mt. Tambora eruption in 1815?

3. Using all coral-based paleoclimate reconstructions available over the last 400 years, is the tropical oceanic temperature and hydroclimate response to strong volcanic eruptions statistically resolvable from the background variability?

To assess the coral-based climate signal in response to the eruptions, I took publicly available coral geochemical records from the Atlantic, Pacific, and Indian Oceans. I separated the coral geochemical records by proxy (Sr/Ca and $\delta^{18}O$). I then performed a superposed epoch analysis (SEA) on all of the data as well as by regional subsets, and by proxy, centered on different eruptions in the past 400 years. In order to evaluate the hydroclimate response to these eruptions, I repeated the same analysis but used only records that had both Sr/Ca and $\delta^{18}O$. By using records with paired $\delta^{18}O$ and Sr/Ca, I was also able to calculate the $\delta^{18}O_{sw}$ and perform the SEA on that variable to separate the temperature and hydrologic responses to the eruptions, as recorded in the coral geochemical data. To address the three questions stated above, the SEAs were performed on two individual eruptions and on nine of the strongest volcanic eruptions in the past 400 years collectively, all which had a global radiative forcing stronger than that of the 1881 Krakatoa eruption according to Sigl *et al.,* (2015).

Paleoclimate research examining the effects of volcanic eruptions on the climate system traditionally focuses on tree rings and ice cores, with much less work using coral records. This research will fill that gap by testing whether coral records can successfully capture volcanic eruption signals. Additionally, coral records are known to be good recorders of ENSO (Alibert and McCulloch, 1997; Kilbourne *et al.,* 2004). As such, connections between ENSO and natural radiative forcing from volcanic eruptions could be further addressed with validated coral data. Lastly, the research presented here could aid in

better understanding the post-eruption marine vs. terrestrial signals and comparing that to land-sea contrasts in climate models.

Chapter 2: Methods

2.1 Data

Publicly available records of coral-skeletal Sr/Ca and $\delta^{18}O$ were compiled for the analysis. The majority of the data came from the PAGES2k 2.0.0 database (PAGES 2k consortium, 2017) because it provided a readily accessible, quality-controlled dataset with extensive metadata. However, the PAGES2k 2.0.0 dataset focuses on temperature sensitive proxies, excluding records that are primarily salinity-driven. Additional records that were not in the PAGES2k compilation were downloaded in August of 2018 from the NOAA/World Data Service for Paleoclimatology and the Data Publisher for Earth and Environmental Science (PANGAEA) archives to complement the PAGES2k data. Records were selected for inclusion if they had either a Sr/Ca or $\delta^{18}O$ chemical composition, were annually resolved, and had at least ten years of data to perform robust significance tests on decadal to multidecadal scale variability. Records with a monthly, bi-monthly or annual resolution were selected and classified as coming from the Atlantic, Indian, or Pacific Ocean basins. Records were excluded if the data did not overlap with known volcanic events. A total of 45 Sr/Ca, and 67 $\delta^{18}O$ records were used in this study; a full list of data that met the criteria are listed in Appendix A.

2.1 Data Processing

The raw coral geochemistry data were processed into annually resolved, detrended anomalies before analysis for volcanic signals, illustrated conceptually in Figure 2. First, a 200-year locally weighted regression smoothing (LOESS) (Neukom *et al.,* 2018; Berk, 2016) was performed on all records to remove the centennial-scale variability from each of the reconstructions, as exemplified in Figure 3. A climatology was then calculated and

removed for the sub-annually-resolved records using the recently detrended data. The data were detrended prior to the climatology calculation to avoid a possible dampening of the calculated annual cycle by lower frequency variability and subsequent incomplete removal of the cycle when anomalies are calculated. After the sub-annually-resolved records were detrended, they were annualized to climatological (April to March) years, resulting in annual anomalies relative to the mean of each record's entire length. For each record that was annualized, if the volcanic eruption occurred between April-Dec, it kept its original calendar year designation. Whereas if the volcanic eruption occurred between January-March, it would have been assigned to the previous calendar year.

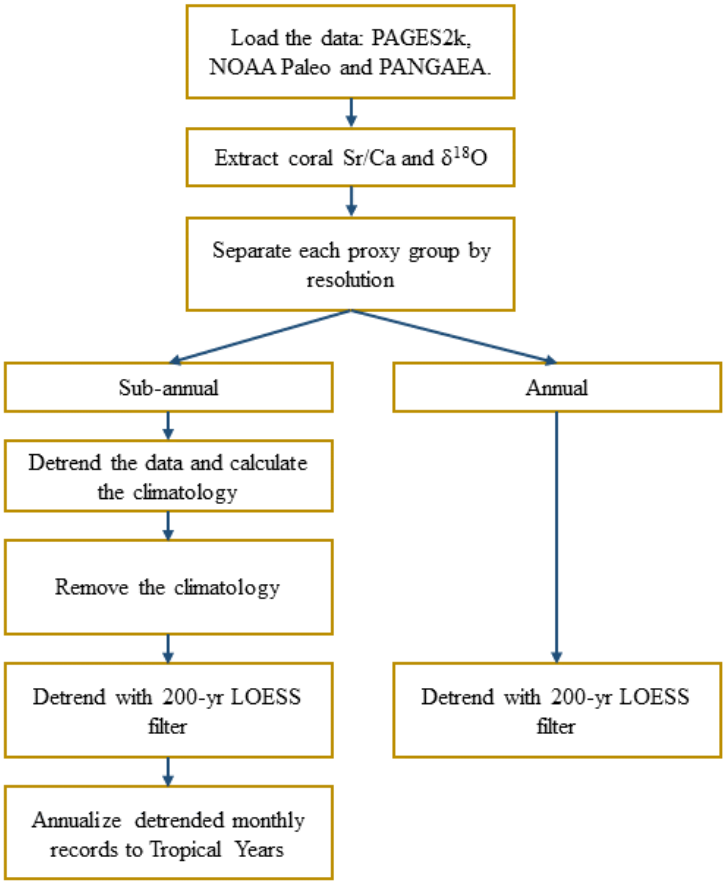

Figure 2. Data Processing Workflow. All data were separated by basins prior to being processes and detrended. This structure was applied to each basin, separately.

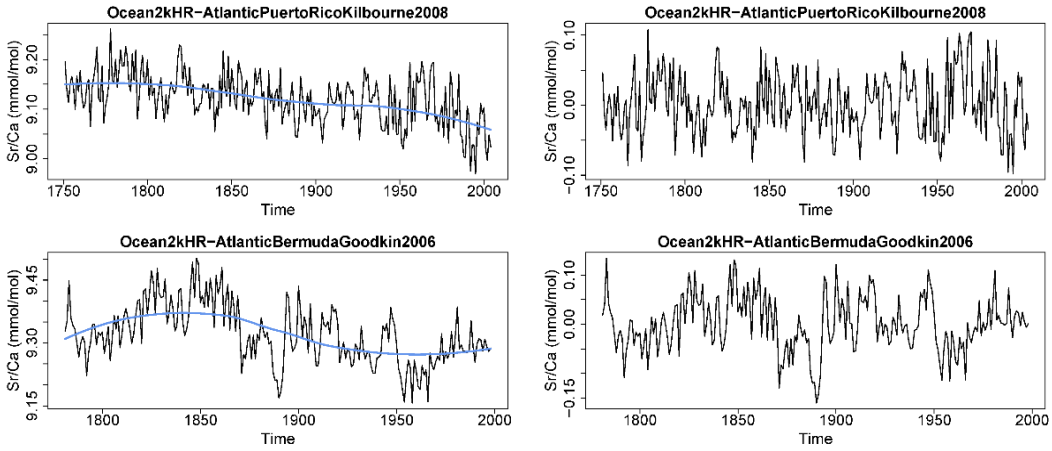

Figure 3. An example of the detrending analysis by 200-year LOESS smoothing on two annually resolved Sr/Ca records from the Atlantic Ocean. The left column shows both records plotted with the LOESS trend and the right column contains the data with the trend (blue line) removed.

2.3 Subsetting the data

Subsets of the data were created to explore how different regions and variables may have responded to volcanic events (see Figure 4 for data groupings). First the data were sorted based on the proxy variable available, Sr/Ca and $\delta^{18}O$. Additionally, records with both Sr/Ca and $\delta^{18}O$ data from the same core were classified as paired records. The paired records take advantage of the fact that Sr/Ca in corals is primarily a function of temperature while $\delta^{18}O$ is primarily a function of temperature and the oxygen isotopic composition of sea water ($\delta^{18}O_{sw}$). By separating the data by proxy, I was able to isolate the sea surface temperature (SST) signals from the mixed SST and sea surface salinity (SSS) signals and observe how each responded the volcanic eruptions in the records. Moreover, separating out the paired records allowed me to examine any seawater $\delta^{18}O$ signal explicitly by removing the temperature variations from the coral $\delta^{18}O$. All of the data were additionally grouped by basin. When treated together, the data represent the global tropics, enabling me

to assess the overall response of the tropical oceans to the volcanic eruptions. Records separated by basin allow for the resolution of regional responses to the volcanic eruption(s).

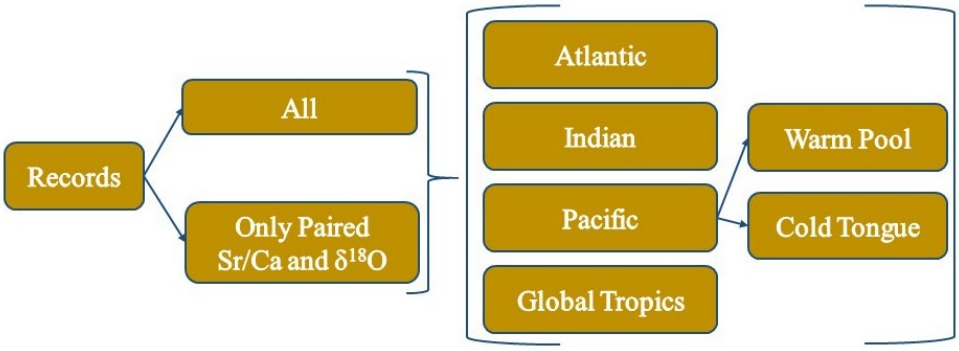

Figure 4. Subsets of coral records analyzed in this study.

Records from the Pacific Ocean were further separated by their expected response to ENSO as it creates SST anomalies of opposite signs in the Eastern and Western portion of the basin. Because of this, they were separated to avoid any possible cancellation of positive and negative ENSO signals in the regional analysis. Records were grouped based on a covariance analysis using NASA Goddard Institute for Space Studies (GISS) surface temperature anomaly data, GISTEMP, with a 1951-1980 base period. GISTEMP data was provided by the NOAA/OAR/ESRL PSD, Boulder, Colorado, USA, from their Web site at https://www.esrl.noaa.gov/psd/, and the version used here uses ERSST v5 (Huang *et al.,* 2017) for the sea surface temperature.

The covariance matrix of the linearly detrended monthly SST anomaly field was calculated over the latitudinal range of −45˚ to 45˚. The first empirical orthogonal function (EOF) of the covariance matrix was used to represent the primary ENSO mode (Figure 5). Coordinates from the Pacific Ocean reconstructions were matched with their corresponding grid values from the first EOF. Records with an EOF value higher than 0 were categorized

as Cold Tongue-correlated, while records with a value lower than 0 were grouped as Warm Pool-correlated.

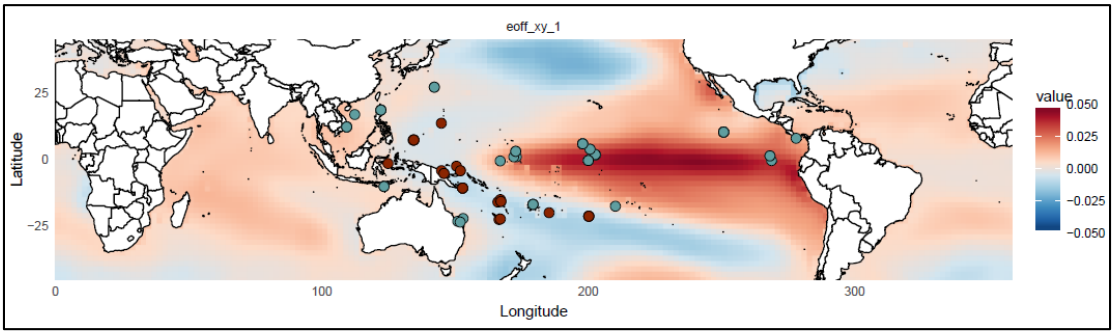

Figure 5. Covariance relationship of SST. The orange and blue dots represent coral records from regions of the ocean with opposite temperature variability on interannual timescales.

2.4 Calculating the seawater $\delta^{18}O$

Various methods exist for calculating the oxygen isotopic composition of seawater ($\Delta\delta^{18}O_{sw}$) from paired Sr/Ca and $\delta^{18}O$ coral geochemical records (McCullough *et al.,* 1994, Gagan *et al.,* 1998, Kilbourne *et al.,* 2004, Cahyarini *et al*., 2008). All of these methods are fundamentally dependent on the $\delta^{18}O$-SST and Sr/Ca-SST calibration relationships. Given the poorly known intercepts of the $\delta^{18}O$-SST and Sr/Ca-SST relationships (Corrège, 2006; Ren *et al.,* 2002), a mean centering method put forth by Cahyarini *et al. (*2008), was used to calculate the $\Delta\delta^{18}O_{sw}$ for the paired records. This was done to omit the intercept in the calculation of the $\Delta\delta^{18}O_{sw}$. The following equation was used:

$$\Delta\delta^{18}O_{sw-center} = \left(\delta^{18}O_{Coral_i} - \overline{\delta^{18}O_{Coral}}\right) - \frac{\gamma_1}{\beta_1}\left(\frac{Sr}{Ca_i} - \frac{\overline{Sr}}{Ca}\right),$$

where $\delta^{18}O_{Coral_i}$ and $\frac{Sr}{Ca_i}$ are the measured coral values while the $\overline{\delta^{18}O_{Coral}}$ and $\left(\frac{\overline{Sr}}{Ca}\right)$ are the calculated means of those values, respectively; β_1 = -0.05 mmol/mol/˚C is the slope of the Sr/Ca -temperature relationship, $\Delta\delta^{18}O_{sw-center}$ is the mean centered oxygen isotopic composition of sea water and $\gamma_1 = -0.2$ per mil/ ˚C is the $\delta^{18}O$ slope against temperature,

chosen as the γ_1 due to its consistency among a wide variety of studies (Epstein *et al.,* 1953; McCulloch *et al.,* 1994; Gagan *et al.,* 1998).

Unlike the $\delta^{18}O$-SST relationship, the Sr/Ca-SST relationship has been characterized with a wider range of values among the published literature, typically ranging from −0.08 to −0.04 mmol/mol/˚C (McCulloch *et al.,* 1994; Gagan *et al.,* 1998; Corrège, 2006; Inoue *et al.,* 2007; Nurhati *et al.,* 2011; Kilbourne *et al.,* 2014; Bolton *et al.,* 2014; Xu *et al.,* 2015). Gagan *et al.,* (2012) argue that different calibration scales should be used dependent on the resolution (seasonal vs annual) of the records. Because of this uncertainty in the Sr/Ca-SST relationship, a range of values for β_1 were tested to explore the sensitivity of the results to the uncertainty in the slope representing a low, medium and high end of the published range, −0.04, −0.05 and −0.08, respectively.

Detrended paired annual Sr/Ca and $\delta^{18}O$ records from the Atlantic, Indian and Pacific Ocean were used to calculate the three $\Delta\delta^{18}O_{sw}$, one for each value of β_1 (an example can be seen in Figure 6). Although the magnitude of the results varied by the value chosen for β_1 (Figure 6), the overall shape of the curves remained the same. Recognizing that the magnitude of any results is fundamentally determined by the choice of β_1, I chose to simplify my analysis using a single value from the mid-range of potential values with −0.05 mmol/mol/˚C as my β_1.

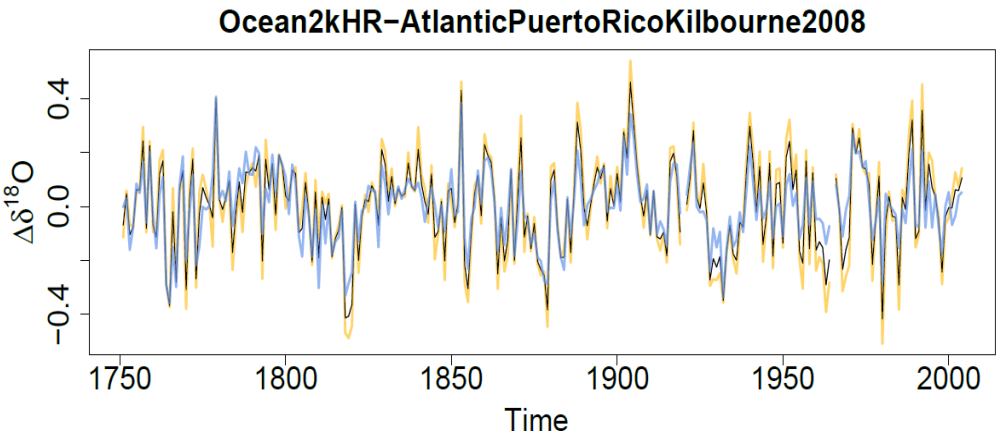

Figure 6. Understanding the effects different Sr/Ca-temperature slopes on $\Delta\delta^{18}O_{sw}$ calculated from a coral record in the Atlantic Ocean. The yellow line represents the parameter $\Delta\delta^{18}O_{sw} = -0.04$, while the black and blue lines are representative of the -0.05 and -0.08 respectively. Minimal change for the magnitude while the shape of the results remained the same for all three values tested.

2.5 Statistical Analysis

The average response of the coral geochemical records to large volcanic events since 1640 CE was assessed by a non-parametric superposed epoch analysis (SEA). For each analysis, I identified the largest, independently determined, stratospheric eruption(s) of the past 400 years (Table 1) and determined the length of the period to observe. The length varied by SEA and was chosen to explore a robust decadal to multidecadal response to the eruption(s). For each record, I removed the mean of the years leading up to the eruption to standardize the anomalies and minimize the influence of non-volcanically induced decadal and/or multidecadal climate variability. The response to a volcanic event was obtained by calculating a median and 95% CI from records stacked together with the volcanic event years superimposed. The 95% CI was calculated for each year of the epochs that made up the SEA by assuming a binomial distribution and obtaining its inverse cumulative density function. This 95% CI was done but was not used in the overall testing of the statistical significance of the eruptions with the SEA's as it was not relevant to the null hypothesis

(H_0) testing; it was done for completion purposes. The median response serves as an estimate of the tropical oceanic temperature and hydroclimate response to the eruption(s) as recorded in coral skeletal chemistry.

*Table 1. All major eruptions that took place since 1640 CE chosen from Sigl et al., (2015). Year chosen and GVF taken from Sigl et al. 2015**

Year CE*	GVF W[m^{-2}]*	Estimated Time of Eruption	Volcano	Location	References
1991	−6.49	1991	Mt. Pinatubo	Philippines	McCormick and Veiga, 1992
1884	−5.48	1883	Krakatoa	Indonesia	Crowley *et al.,* 1997; Fischer *et al.,* 2007
1836	−6.57	1835	Cosigüina	Nicaragua	Fischer *et al.,* 2007; Adams *et al.,* 2003, Amman *et al.,* 2003
1832	−6.46	1832	Unknown	Unknown	Gao *et al.,* 2008; Garrison *et al*., 2018
1815	−17.20	1815	Mt. Tambora	Indonesia	Gao *et al.,* 2017; Fischer *et al.,* 2007
1809	−12.01	1808-10	Unknown	Unknown	Guevara-Murua *et al.,* 2014
1783	−15.49	1783-84	Laki	Iceland	Thordarson and Self, 2003
1695	−10.24	1695	UE-1695		Sigl *et al.,* 2015
1641	−11.84	1640	Parker	Philippines	Iles *et al*., 2013; Fischer *et al.,* 2007

Investigating the statistical importance of the signals identified in the SEA, I created a null set of data that can be used to test the following hypothesis:

- H_0: There is no association between volcanic events and climate anomalies.
- H_A: Volcanic event years display climate anomalies compared to non-volcanic years.

With this, I explored if, for any given year, do we expect an anomaly with a magnitude (positive or negative) as great as the anomalies generated from the population

of non-volcanic year SEAs? What was the likelihood that anomalies identified from the volcanic event SEAs came from the underlying distribution of non-volcanic SEAs?

To create a set of data not influenced by volcanic forcing that could be used as a null set, I removed the year of each volcanic eruption from every coral record, as well as the ±2 years around the eruption, to remove the data that could potentially have the strongest volcanic signal. Years were removed before and after the eruption year to account for the possibility of age model errors in the coral records that could put a volcanic event at a slightly different time in the coral data than it actually occurred.

A matrix was then created from the non-eruption data by randomly selecting (with replacement) from the remaining years. The number of columns of the matrix depended on the length chosen for the original SEA, while the number of rows were dependent on the number of eruptions originally identified in each record, so that each H_0 SEA had the same number of years and records stacked as the controlled (eruption-year) SEA being compared. All records in the matrix had their pre-eruption mean subtracted from the data, same as was done for the eruption years, and a median SEA was calculated. This process was repeated a total of 100 times, creating an array of 100 median SEAs. A 95% confidence interval (CI) was calculated for each year of the epochs based on the 100 iterations of the SEA using 97.5% and 2.5% quantiles to obtain a measure of the background signal expected due to non-volcanically forced tropical oceanic temperature and hydroclimate variability. This process was repeated regionally for each iteration of the analysis.

It is important to note that for these two SEA variations (with and without eruptions) the goal was to identify substantial results/anomalies in the data. These analyses are not to be confused with a test of their significance.

2.6 Volcanic Events Studied

A regional SEA was performed for the 1991 Mt. Pinatubo eruption (global volcanic forcing (GVF) of -6.49 W[m^{-2}]) (Table 1) to test the sensitivity of capturing individual volcanic event signals in coral geochemical records. The eruption was chosen because it was the most recent large event, so there are many available proxies and the age models are fairly certain because the event lies in the top portion of the skeletons. Additionally, being the most recent event, we have good instrumental data about the response of the climate system to the event. The only drawback is that, although Mt. Pinatubo was a climatically significant event, it did not produce an exceptionally large radiative perturbation, and the relatively weak signal may be difficult to detect in coral skeletal geochemistry records. The analysis followed the same methodology as stated in section 2.5. Time periods of −5: +10 years were chosen to look at the interannual-scale variability in the data. For these periods, the year of eruption was represented by the year 0 in the SEAs. This was done regionally, by proxy, for all and paired records. It was also done for the global tropics to look at the pantropical response of the records to the eruption, while testing the effect of including/excluding Pacific Cold Tongue correlated records.

To account for the possibility that the coral records could not capture a signal as small as the 1991 Mt. Pinatubo event, the SEA was repeated on the 1815 Mt. Tambora eruption (GVF of −17.20 W[m^{-2}], which had the largest GVF out of all the eruptions that occurred since 1640 CE. Time periods of −5: +13 were chosen to include the 1809 "Unknown" eruption (GVF of -12.01W[m^{-2}]) and account for any influence it might have had on the climate surrounding the 1815 event. For this reason, the SEA was centered on

the 1809 eruption and a regional and pantropical SEA was done to observe the temperature and hydroclimate response of all and paired records to both eruptions.

While the SEA followed the methods established in Section 2.5, the non-eruption SEAs deviated from that methodology in that the years surrounding both the 1809 and 1815 eruptions were removed for the H_0 set. This action ensured no volcanic influence was present in the calculation of the non-eruption SEA.

Just as any one year may not perfectly represent the climatological norms, any single eruption may have its own characteristic impacts on the climate system. To explore the overall response of the climate system to the canonical forcing of volcanic eruptions, a SEA was performed on all time intervals corresponding to major eruptions that took place since 1640 CE. Merging all available data had the added benefit of maximizing the signal to noise ratios by averaging out the noise in the records. Due to the length of the coral records used in this study, a total of nine volcanic eruptions (Table 1), all of which had a GVF higher than that of the 1883 Krakatoa eruption (GVF of -5.48 W[m^{-2}]), were selected from Sigl *et al*., 2015. Eruption years were selected from Sigl (2015) because they used the cosmogenic nuclides ^{14}C and ^{10}Be in tree-ring and ice core data to improve the estimated timing of volcanic events during the last 2,500 years. Their work addressed earlier inconsistencies between the timing of volcanic eruptions and their effects on the climate system.

I selected a time interval of −5: +30 years to characterize the initial climate state and capture any effects of eruptions on multidecadal variability which has been proposed for the Atlantic sector (Otto-Bliesner *et al.,* 2016). I calculated the median SEA for all eruptions and the non-eruption SEA as described in Section 2.5. The median response of

coral records calculated in the SEA served as an estimate of the canonical tropical oceanic temperature and hydroclimate response of all coral records to all nine volcanic eruptions.

2.7 Estimating Temperature Signals

The SEAs describe the magnitude of the signals in a geochemistry space; as such, it is necessary to translate the signals to temperature to understand their potential climate signal. To calculate the relative temperature, change from the SEA anomalies, I used the same calibration slopes that were used to calculate the seawater $\delta^{18}O$ (section 2.5). As stated in section 2.4, I used a value of −0.05 mmol/mol/˚C as the slope for the Sr/Ca-temperature relationship, whereas −0.2 per mil/ ˚C was used as the $\delta^{18}O$ slope against temperature. The $\delta^{18}O$ slope value of −0.2 per mil/ ˚C was chosen based on its use and consistency throughout a wide range of studies. Whereas I chose the Sr/Ca-SST slope from an uncertainty analysis, I performed on a variety of values (−0.08 to −0.04) cited in the coral paleoclimate literature. Ultimately, a value of −0.05 mmol/mol/˚C was chosen from the mid-range of potential Sr/Ca-SST relationship values because the overall shape/behavior of the curves remained the same no matter which slope is used.

Chapter 3: Results

3.1 Significance of the results

For each of the SEAs conducted, I considered significant only median SEA results exceeding (above or below) the H_0 envelope, illustrated in figures 7-15 as a yellow band. For those instances, we reject the H_0 with a critical p-value of 0.05. Signals that barely surpassed the yellow band were not considered substantial unless there were similar signals from other relevant data, since one expects the 95% confidence threshold be breached about 5% of the time even when no true signals are present. Although the median results were occasionally above the range expected from normal climate variability, and I chose to interpret those signals, the 95% CI on those medians never exceeded the H_0 expected range.

3.2 SEA: 1991 Mt. Pinatubo

I used a range of 40 (Sr/Ca) to 53 ($\delta^{18}O$) record segments to calculate pantropical SEA's for the 1991 Mt. Pinatubo eruption from coral $\delta^{18}O$, Sr/Ca, and $\Delta\delta^{18}O$ data (Figure 7). Twenty corals had both Sr/Ca and $\delta^{18}O$ data for the paired-data comparison and analysis of $\Delta\delta^{18}O$ (Figure 8). The analysis period spanned 1986-2001. The magnitude of the background variability calculated from the non-eruption years (yellow shading in the figures) is directly related to the number of record segments in the analysis, such that a larger (smaller) number of record segments produced a smaller (larger) magnitude of background variance expected.

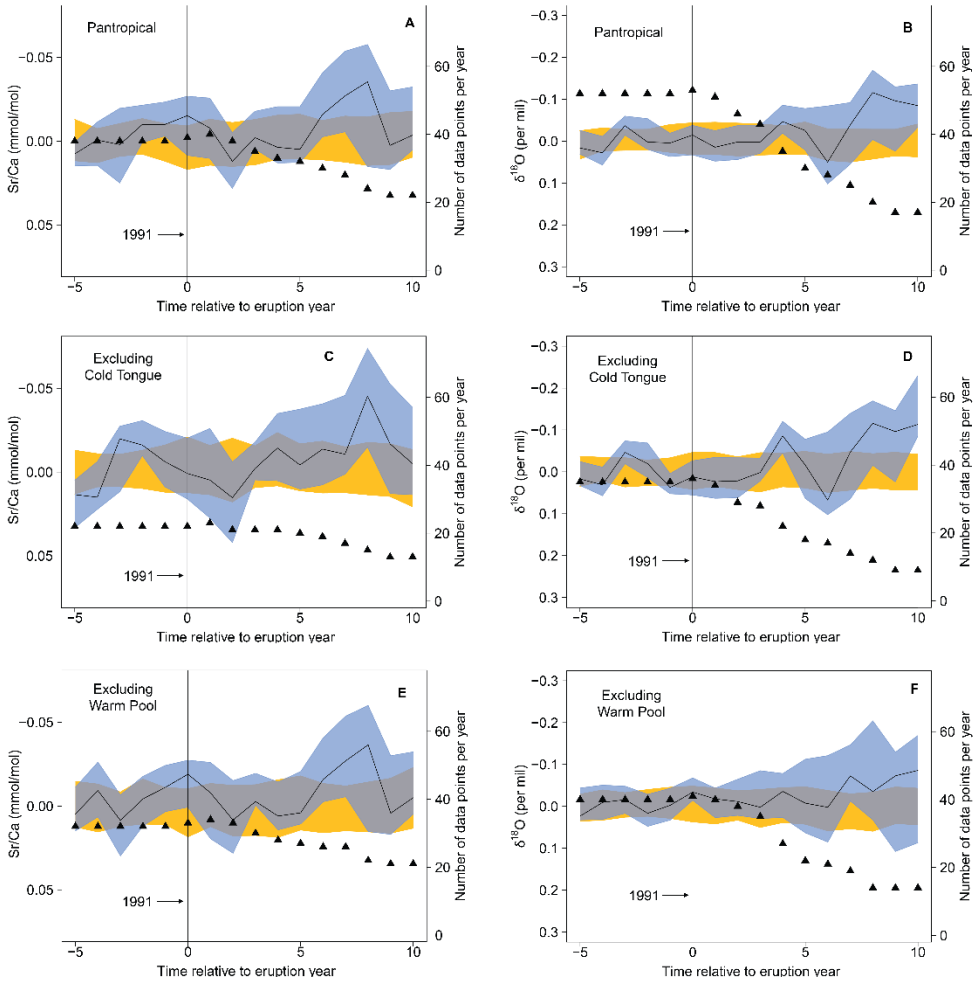

Figure 7. The response of coral Sr/Ca and $\delta^{18}O$ to the 1991 Mt. Pinatubo eruption using all coral records available. The Warm Pool and Cold Tongue from the Pacific Ocean represent the records as they were correlated to ENSO in the instrumental SST record, not the geographical ranges. The black line is the median response to the volcanic eruptions and the blue shaded area represents its 95% CI. The yellow shaded area represents the 95% CI for 100 SEA calculations using randomly selected non-eruption years from the same records. The vertical line at year zero represents the year of eruption, while the black triangles represent the number of coral records available for each year (right axis). H_0 is rejected at pcrit = 0.05 for year −3 for Sr/Ca and $\delta^{18}O$ by excluding the Pacific Cold Tongue records. The significant signal for Sr/Ca and $\delta^{18}O$ around year +7 to +9, is attributable to the strong El Niño and La Niña events of the late 1990s.

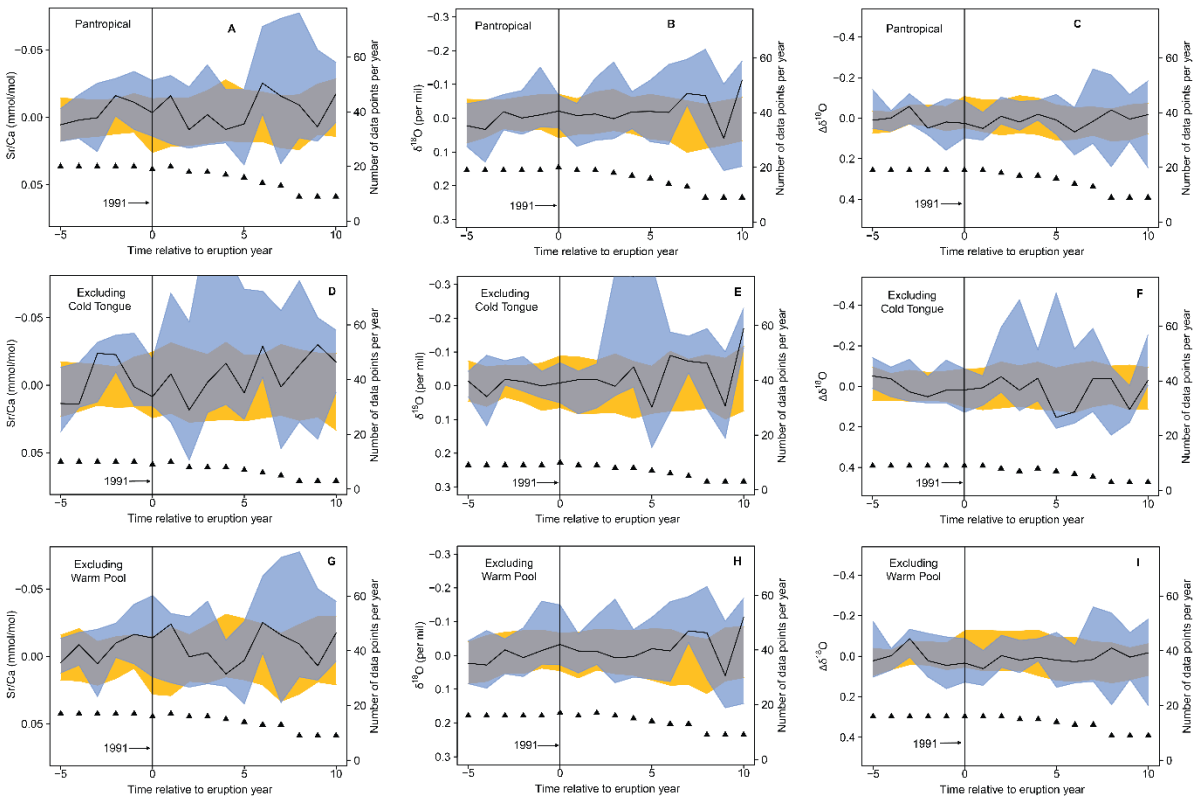

Figure 8. The response of coral Sr/Ca, $\delta^{18}O$ and $\Delta\delta^{18}O$ to the 1991 Mt. Pinatubo eruption using all paired coral records available. The symbol description is the same as in Figure 7. The Warm Pool and Cold Tongue from the Pacific Ocean represent the records as they were correlated to ENSO, not the geographical ranges. No significant difference found by including/excluding the Pacific Cold Tongue and Warm Pool records. Note the fewer number of records (data points) available with paired Sr/Ca and $\delta^{18}O$ than for all other datasets.

For example, the pantropical analysis with all $\delta^{18}O$ records (Figure 7) contained 53 record segments and the pantropical analysis with just the paired (Figure 8) $\delta^{18}O$ records contained 20 record segments. This resulted in average 95% confidence ranges of ± 0.03 ‰ and ± 0.06 ‰, respectively. As stated in the Methods section (2.5), the influence of ENSO-sensitive Pacific records on the pantropical SEA was tested by removing sites with positive and negative SST correlations to ENSO during the 20th century, associated with the eastern Pacific Cold Tongue and western Pacific Warm Pool respectively. This resulted in SEA's covering three spatial regions for the $\delta^{18}O$ and Sr/Ca data available during the Mt. Pinatubo analysis period: 1. Pantropical, 2. Warm Pool excluded and 3. Cold Tongue excluded. The same analyses were repeated for the paired $\delta^{18}O$, Sr/Ca, and $\Delta\delta^{18}O$ coral data.

In the immediate years surrounding the 1991 eruption, only the Sr/Ca data from around the tropics showed significant anomalies as the SEA for those years exceeded the H_0 band; similar signals were not found in the $\delta^{18}O$ data (Figure 7). A pantropical Sr/Ca signal of −0.015 mmol/mol (with a 2-sigma range of −0.026 to 0.009 mmol/mol) exists in the year of the eruption (Figure 7a). The median Sr/Ca SEA signal surpasses the null hypothesis envelope, with a temperature increase of 0.3 ˚C. A similar Sr/Ca signal of −0.018 mmol/mol (with a 2-sigma range of −0.027 to 0.001 mmol/mol) exists in the analysis that excluded the Pacific Warm Pool (Figure 7e); this translates to a 0.36 ˚C increase in temperature in the year of the eruption. The slightly stronger signal when excluding Pacific Warm Pool data indicates that the Warm Pool region did not have a warming signal. Similar SEA analyses of the paired Sr/Ca and $\delta^{18}O$ data (Figure 8) did not

have significant signals surrounding the Pinatubo eruption as the number of data points available dropped substantially and the uncertainty bounds grew proportionately.

Apart from the immediate years surrounding the 1991 eruption, there were strong coherent signals present in the data before and after the volcanic event took place. Strong Sr/Ca and $\delta^{18}O$ negative anomalies were detected in the pantropical analysis using all available data beginning in year +6 (1997) and extending through year +9 (2000) after the 1991 eruption took place (Figure 7, a and b). These signals remained when either the Pacific Cold Tongue or Warm Pool records were excluded (Figure 7, c-f). All three Sr/Ca SEA's presented signals in comparable magnitude (Figure 7 a, c and e), with a Sr/Ca pantropical signal of −0.035 mmol/mol (95% CI of −0.057 mmol/mol to 0.015 mmol/mol) (Figure 7 a). Whereas the $\delta^{18}O$ pantropical SEA produced a signal of −0.11 ‰ (95% CI −0.004 ‰ to −0.16 ‰, N=20) during 1999, (Figure 7b). These pantropical Sr/Ca and $\delta^{18}O$ signals translate to a 0.7 ˚C and 0.55 ˚C increase in temperature respectively.

Comparable, though smaller increases in temperature were present in the pantropical paired records for both Sr/Ca and $\delta^{18}O$. Sr/Ca had a signal of −0.025 mmol/mol (95% CI of −0.002 mmol/mol to −0.067 mmol/mol) at year +6 (1997), representative of a 0.5 ˚C increase of temperature (Figure 8 a). The strongest $\delta^{18}O$ signal of −0.07 ‰ took place during years +7 (1998) to +8 (1999), with a two-sigma range of -0.038 ‰ to −0.17 ‰) indicative of a 0.35 ˚C temperature increase, if interpreted in terms of temperature alone. The same signals were present when excluding the Pacific Warm Pool records for both Sr/Ca and $\delta^{18}O$, though not when the Cold Tongue records were excluded, indicating that warming in Cold Tongue-associated regions may have contributed to the signal.

Analogous warming signals were also present in 1988 for all and paired records, three years before the 1991 eruption took place. A slightly larger warming signal is seen at that time in the Sr/Ca and $\delta^{18}O$ data when the Pacific Cold Tongue records are excluded (Figure 7, c-d), indicating that the warming signal was indeed pantropical and not just due to warming of the eastern Pacific during ENSO. The magnitude of the 1988 signals are −0.019 mmol/mol and −0.046 ‰ (VPDB), translating to 0.38˚C and 0.23˚C respectively, if the entire $\delta^{18}O$ signal was temperature. Paired SEAs had only one significant Sr/Ca signal that lasted from 1987-1988 (lags −3 and −4 in the x-axis), with a value of −0.022 mmol/mol (Figure 8 d), when excluding the Pacific Cold Tongue records.

In addition to the above-described analyses, the data were broken out into ocean basin regions for all (Appendix B. 1) and paired (Appendix B. 2) records but graphs of the data are not included in this main thesis text. Few records satisfied our criteria for the regional-scale analysis, leaving only 4-19 (Appendix B. 1) and 1-10 (Appendix B. 2) records for analysis. With so few records, not enough data remained to reasonably estimate of the background climate variability, nor to generate reasonable uncertainty bounds on the median eruption signal.

3.3 SEA: 1809 'Unknown' and 1815 Tambora Eruptions

The earlier timing of 1809 and 1815 eruptions resulted in fewer coral records available to calculate the pantropical SEAs for all (Figure 9) and paired (Figure 10), compared with the 1991 Mt. Pinatubo eruption. I used a range of 13 (Sr/Ca) to 23 ($\delta^{18}O$) record segments for the pantropical SEAs, and only six records for the paired analyses. This decrease in records and record segments resulted in more background variability. The increased background variability is visible in these data by comparing the analyses using

all records in Figure 9 versus just the paired records in Figure 10. I used the same types of SEAs as in the Mt. Pinatubo analysis covering three spatial regions for all and paired $\delta^{18}O$, Sr/Ca, and $\Delta\ \delta^{18}O$ available coral data for the 1804 to 1822 period.

A distinct cooling signal was identified in the Sr/Ca SEA analyses one year before the 1809 eruption (Figure 9a, c, e), despite the relatively low number of coral records available. The result was not sensitive to the exclusion of the Warm Pool or Cold Tongue associated records. The pantropical Sr/Ca SEA signal had a value of 0.036 mmol/mol, with 95% confidence that the true median response lies between 0.007 mmol/mol to 0.045 mmol/mol (Figure 9a). This signal translates to a −0.72 ˚C temperature anomaly with 95% likelihood that the true signal lies between −0.9 ˚C and −0.13 ˚C.

The $\delta^{18}O$ data produced only one peak that barely exceeded the H_0envelope, which occurred when Cold Tongue records from the Pacific Ocean were excluded (Figure 9 d). This response is considered as a potentially typical spurious peak as one would expect 5/100 with a 95% confidence-level uncertainty envelope, as it was not present in any other analyses of the $\delta^{18}O$ data. Thus, the results of the $\delta^{18}O$ SEA analyses indicate no substantial $\delta^{18}O$ signals were detected above the background climatic variability for the 1809 and 1815 eruptions.

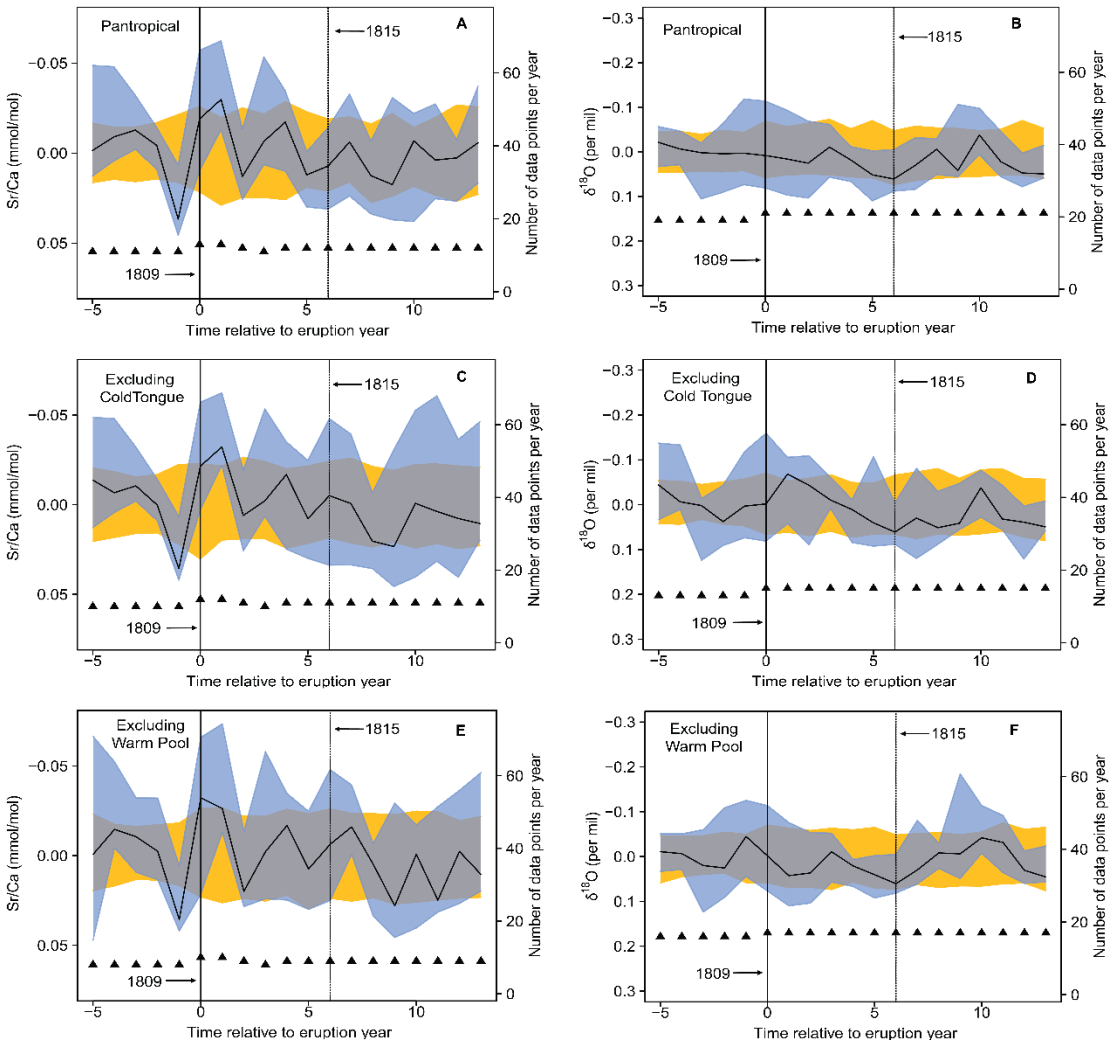

Figure 9. The response of coral Sr/Ca and $\delta^{18}O$ to the 1809 "Unknown" and 1815 Mt. Tambora eruptions using all coral records available. The symbol description is the same as in Figure 7. The Warm Pool and Cold Tongue from the Pacific Ocean represent the records as they were correlated to ENSO over the 20th Century, not the geographical ranges. Significant cooling is detected the year before the 1809 eruption, for all three pantropical scenarios for Sr/Ca. There was a small suggestive signal for $\delta^{18}O$ that was not significant against the null hypothesis testing when excluding records from the Pacific Cold Tongue.

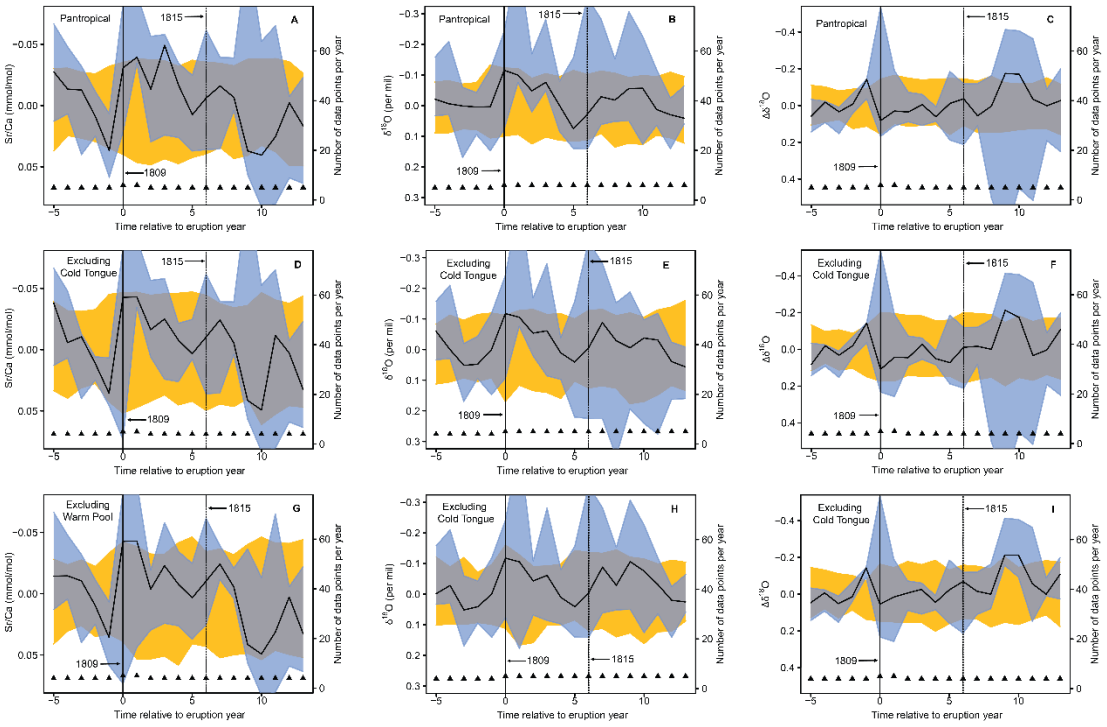

Figure 10. The responses of coral Sr/Ca, $\delta^{18}O$ and $\Delta\delta^{18}O$ to the 1809 "Unknown" and 1815 Mt. Tambora eruptions using all paired coral records available. The symbol description is the same as in Figure 7. The Warm Pool and Cold Tongue from the Pacific Ocean represent the records as they were correlated to ENSO, not the geographical ranges. A one-year lead of the large anomaly relative to the year of the eruption is consistent in all three paired pantropical scenarios for both the 1809 and 1815 eruptions suggestive of a potential age model error in the coral records. The large variance in the figures is a result of the limited number of data points per year and do not represent the uncertainty of the results.

Similar to the results using all of the data, the strongest signal in the paired data analysis was a large positive Sr/Ca anomaly in the year before the 1809 eruption and a subsequent rapid decrease in Sr/Ca the year of the event (Figure 10). The signal is consistent when Cold Tongue records or Warm Pool records from the Pacific Ocean were excluded (Figure 10 d and g). A weaker drop in temperature relative to the surrounding years occurs also the year before the Tambora eruption in 1815, but the signal is not as strong and there are no significant geochemical anomalies. The $\delta^{18}O$ decrease was weaker and less coherent, but the $\Delta\delta^{18}O$ signal was more robust, due to the influence of the strong Sr/Ca signal. The $\Delta\delta^{18}O$ also presented an increase in its variance after the year of the eruption(s) (Figure 10 c, f, i). More investigation is needed to understand this increase in variance, if it is an artifact of noisy data, or if it is a real signal and could have implications for changes in the hydrologic cycle after an eruption.

Regional SEA's were also done for all (Appendix C. 1) and paired (Appendix C. 2) records that included the 1809 and 1815 eruptions. Only 1-8 and 1-2 records were available these analyses respectively. The lack of records per region prevented the calculation of the 95% CI of the median response to both volcanic eruptions for which the figures were not included in this chapter.

3.4 SEA: All Nine Eruptions

To maximize the signal to noise ratios, I focused on the nine most energetic eruptions since 1640 C.E. I used a range of 32 (Sr/Ca) to 59 ($\delta^{18}O$) records and record segments to calculate the SEAs using all of the data, and 15 for the paired SEA(s). Similar to the analyses of the Pinatubo event, and the early 1800's eruptions, the uncertainty envelope on the background variability decreased as the number of records used for these analyses

increased. As in the prior sections, SEAs covering three spatial regions were carried out for all and paired $\delta^{18}O$, Sr/Ca, and $\Delta\delta^{18}O$ available coral data. Unlike the prior sections, there were enough data for a useful analysis of the data sub-set into regions, Atlantic, Indian, Pacific Warm Pool and Pacific Cold Tongue.

A clear signal emerged in the $\delta^{18}O$ data from the SEA using all data sets and all 9 eruptions (Figure 11 b, 9b). Figure 11 contains panels with the same size axes as in Figure 13 and 15, so that the reader can visually compare signals between the different analyses. The axes are adjusted in Figure 12 (and Figure 14) so that the reader can better see the described signal.

The primary signal manifests as an increase in $\delta^{18}O$ (Figure 11 and 12 b, d, f) at the time of the eruption, with a prolonged warm anomaly 10-15 years later. The signal is similar when the Warm Pool associated records are removed and when the Cold Tongue records are removed (Figure 11 and 12, d and f). However, the cooling and subsequent warming signals were less defined after removing the Warm Pool records (Figure 11 and 12 f), hinting that the signal might be stronger in the Warm Pool region. Contrary to the $\delta^{18}O$ SEAs, the Sr/Ca analysis contained no clear signals, no matter the subset of data used (Figure 11 and 12 a, c, and e).

The pantropical $\delta^{18}O$ SEA (Figure 11 and 12 b) cooling signal in the year of the eruption was +0.044 ‰ (with a 95% CI of 0.008 ‰ to 0.059 ‰). As previously mentioned, excluding Pacific Cold Tongue and Warm Pool records resulted in colder/dryer conditions for $\delta^{18}O$ data, the year of the event (Figure 11 and 12 d, f). The strongest signal identified was of 0.049 ‰ (with a two sigma range of 0.066 ‰ to 0.008 ‰) when excluding the Cold

Tongue correlated records (Figure 11 and 12 d). This signal is representative of a 0.25 ˚C decrease in temperature, if the entire signal is interpreted in terms of temperature.

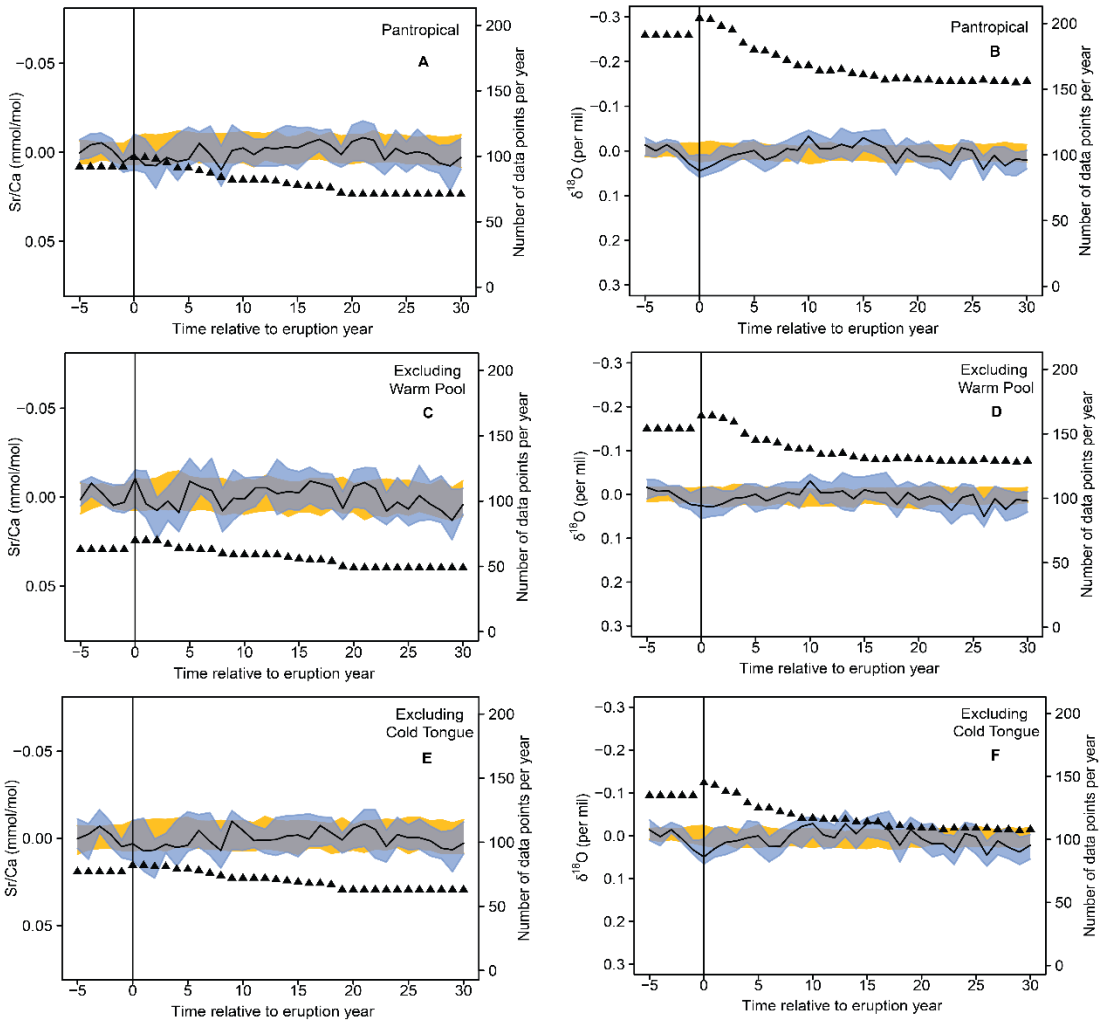

Figure 11. The response of coral Sr/Ca and $\delta^{18}O$ to the 9 strongest eruptions since 1640 CE using all coral records available. The symbol description is the same as in Figure 7. The Warm Pool and Cold Tongue from the Pacific Ocean represent the records as they were correlated to ENSO, not the geographical ranges. No significant difference is seen by including or excluding the Pacific Cold Tongue records. Slight cooling for $\delta^{18}O$ is insignificant against the null hypothesis that similar results could be obtained from non-eruptions years.

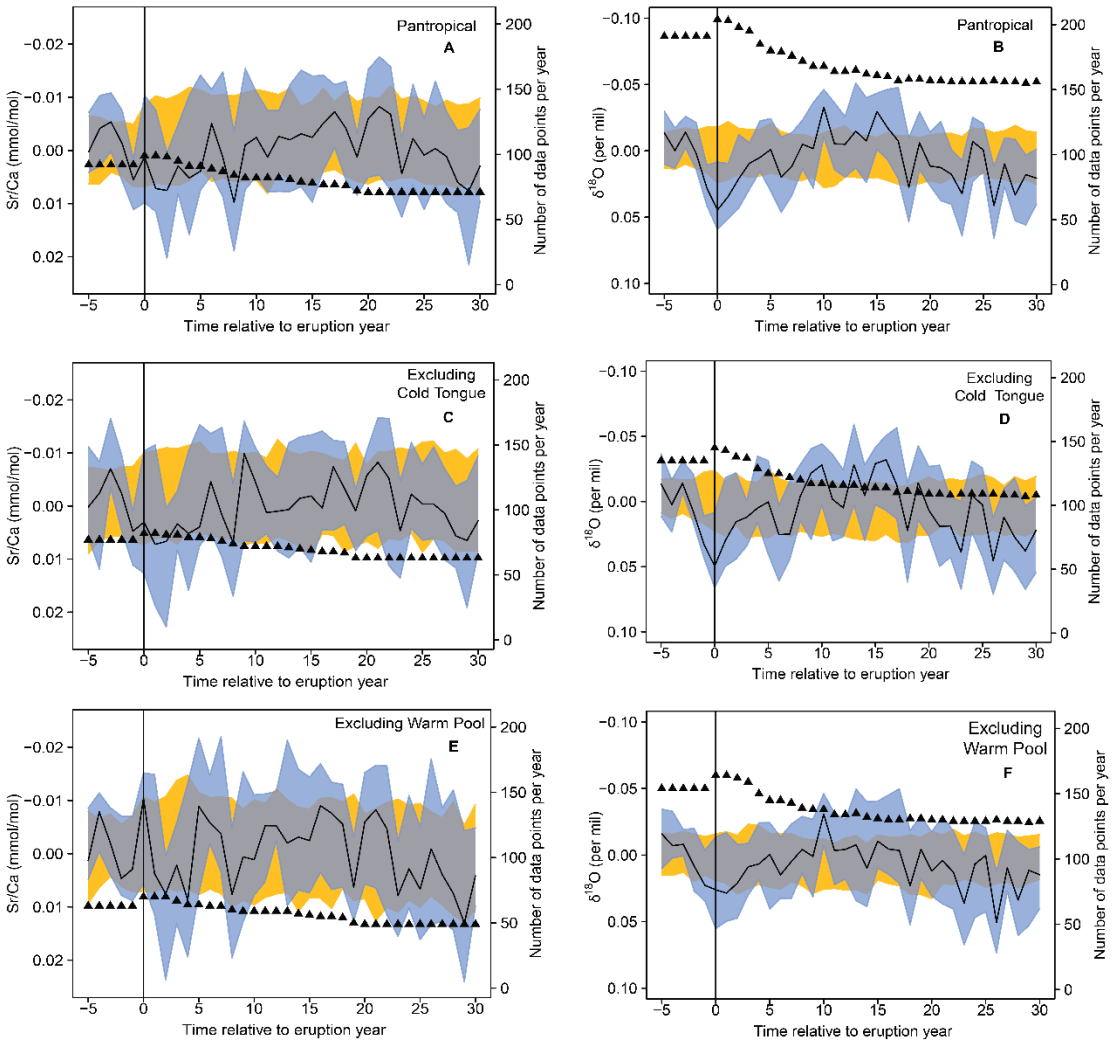

Figure 12. All records/eruptions new limits response of coral Sr/Ca and $\delta^{18}O$ to the 9 strongest eruptions since 1640 CE using all coral records available with new y-limits representative of a 0.5 ˚C change in temperature. The symbol description is the same as in Figure 4. The Warm Pool and Cold Tongue from the Pacific Ocean represent the records as they were correlated to ENSO, not the geographical ranges. Slight cooling for Sr/Ca is insignificant against the null hypothesis that similar results could be obtained from non-eruptions years. A ~0.245 ˚C decrease in temperature is identified, the year of eruption(s) for $\delta^{18}O$.

Paired SEAs showed much variability throughout the selected 36-year period (Figure 13 - 14). A few data points peaked above the thresholds defined by the background climate (yellow band). Still, there was nothing that seemed consistent between different subsets of the data and no signals that rose or dipped beyond that threshold substantially enough to seem truly significant. Additionally, regional SEAs were done for all and paired coral records available. I found no significant signals in the regional paired records SEA for Sr/Ca, $\delta^{18}O$, and $\Delta\delta^{18}O$ (Appendix: Figure E). All paired results fell within the 95% CI of the non-eruption years SEA performed from the same coral-based records.

Each ocean basin behaved slightly differently in the regional SEA analysis. The data suggest cooling/drying in the Pacific Warm Pool in the nominal event year, evidenced by increases in both Sr/Ca and $\delta^{18}O$ (Figure 15). The western Pacific $\delta^{18}O$ produced a signal of 0.074 ‰ (with a two-sigma confidence range of 0.030 ‰ to 0.093 ‰, Figure 15 f) the year of the eruption. This signal was representative of a 0.37 ˚C decrease in temperature, if interpreted entirely as a temperature change. Pacific Warm Pool records for Sr/Ca showed a weaker 0.19 ˚C temperature decrease the year before and after the eruption, with a signal of 0.013 mmol/mol (95% CI of 0.003 mmol/mol to 0.023 mmol/mol). The positive Sr/Ca and $\delta^{18}O$ anomalies in the Warm Pool seemed to leak into other years, with distinctly positive anomalies before and after. The eastern Pacific Ocean did not reflect the same behavior as the western Pacific. The Sr/Ca (Figure 15 g) for this region was characteristic of much noise in the data. In contrast, the $\delta^{18}O$ from the eastern Pacific follows a similar response as in the western Pacific, although with a much weaker effect.

The regional data further showed the negative $\delta^{18}O$ anomaly 10-15 years after the year of the eruption. The Pacific Warm Pool had an average signal of −0.037 (with a 95%

CI of −0.086 to 0.01) for the years +9 to +16 after the volcanic event(s) took place. The Cold Tongue correlated records in the Pacific Ocean contained a long-term warming, or isotopic shift, similar in timing yet weaker than that of the Warm Pool, with an average magnitude of −0.016 ‰ (with a two-sigma confidence range of −0.066 ‰ to 0.027 ‰, Figure 15 h) the year of the eruption. The Indian Ocean followed in terms of strength, with an average magnitude of −0.005 ‰ (95% CI of −0.041 ‰ to 0.032 ‰). It is important to note that although there is a warming signal present, it does not clear the null hypothesis testing significance level. For the years +9 to +16, these signals translate to a warming of 0.2 ˚C, 0.08 ˚C, 0.03 ˚C for the Warm Pool, Cold Tongue, and Indian Ocean, respectively. Contrary to the other basins, the $\delta^{18}O$ records from the Atlantic Ocean (Figure 15, a-b) showed no distinct signal for the eruption year, nor for the 10-15 years after the eruption(s) took place. Signal-to-noise ratios could cause the regional responses to all 9 of the selected eruptions in each basin.

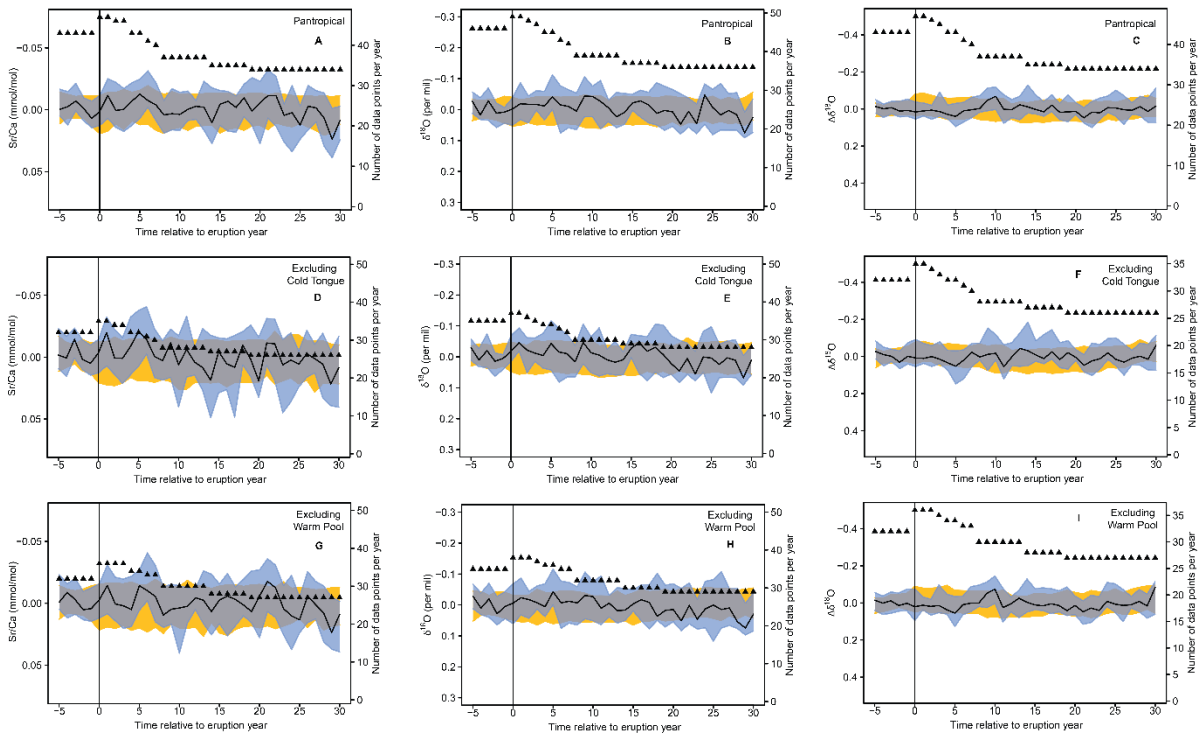

Figure 13. The response of coral Sr/Ca, $\delta^{18}O$ and $\Delta\delta^{18}O$ to the 9 strongest eruptions since 1640 CE eruptions using paired coral records available. The symbol description is the same as in Figure 4. The Warm Pool and Cold Tongue from the Pacific Ocean represent the records as they were correlated to ENSO, not the geographical ranges. No significant difference is seen by including or excluding the Pacific Cold Tongue and Warm Pool records.

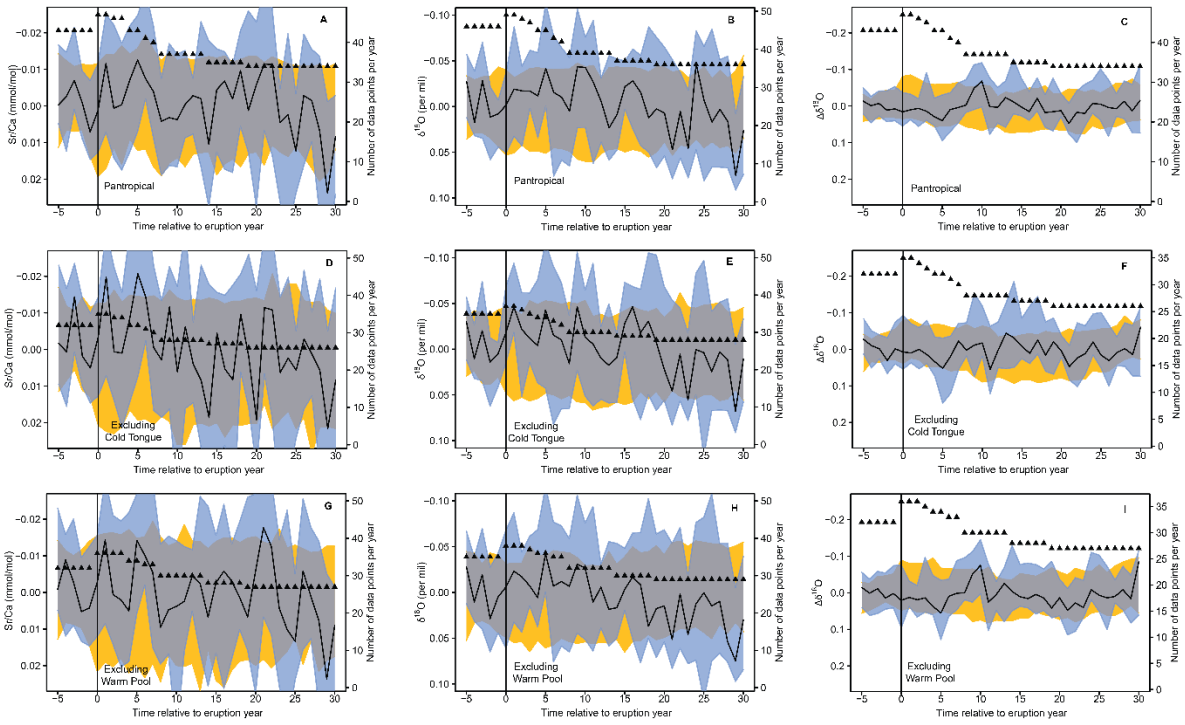

Figure 14. The response of coral Sr/Ca, $\delta^{18}O$ and $\Delta\delta^{18}O$ to the 9 strongest eruptions since 1640 CE eruptions using paired coral records available. The symbol description is the same as in Figure 4. The Warm Pool and Cold Tongue from the Pacific Ocean represent the records as they were correlated to ENSO, not the geographical ranges. A 0.068 increase in temperature is identified for Sr/Ca when excluding records from the Pacific Cold Tongue. No significant difference is seen by including or excluding the Pacific Cold Tongue and Warm Pool records for $\delta^{18}O$ and $\Delta\delta^{18}O$.

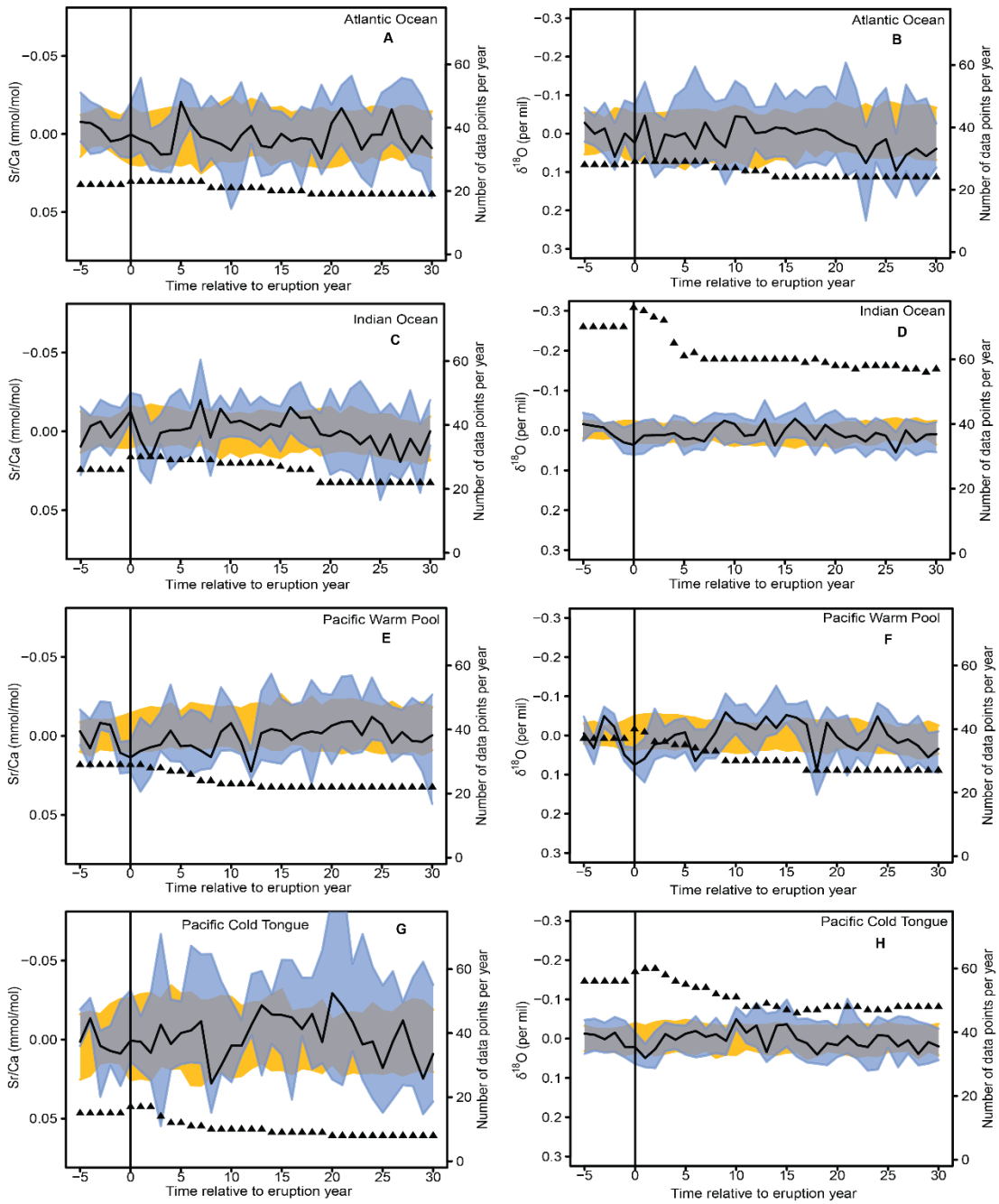

Figure 15. The response of coral Sr/Ca and $\delta^{18}O$, in each tropical ocean basin, to the 9 strongest volcanic eruptions since 1640 CE, using all coral records available. An increase in $\delta^{18}O$ is seen in the years immediately surrounding the volcanic eruptions suggesting slight cooling or drying. The strongest signal identified was seen in the Western Pacific for both proxies while it is not present in the Atlantic region.

Chapter 4: Discussion

4.1 1991 Mt. Pinatubo Eruption

The 1991 Mt. Pinatubo eruption had a GVF of -6.49 W[m^{-2}] (Sigl *et al.,* 2015), with a maximum mean global surface temperature decrease of 0.5 ˚C that peaked in approximately September-December 1992, based on land station and ship-based observations (Parker *et al.,* 1996). The coral Sr/Ca data indicate the opposite signal in the tropics, ~0.3 ˚C warming. One possible explanation as to why there was warming the year of eruption, and why it increased when excluding the western Pacific, is because the 1991 eruption coincided with a weak El Niño event (Kessler and McPhaden, 1995). This aligns with the results, as the warming signal was slightly larger when excluding the western Pacific Warm Pool-correlated records, which are cool during El Niño events, and the warming signal disappeared when excluding the Cold Tongue-correlated records, which are anomalously warm during El Niño events.

The Pinatubo SEA was designed to detect large-scale perturbations to ocean temperature and oxygen isotopic conditions over a particular time period. Thus, in addition to any volcanic signals, ENSO events should be detectable if they occurred during the period chosen for the SEA. Indeed, the most significant anomalies detected in the data occurred during known ENSO events. This is abundantly clear when an index of ENSO is plotted with the SEA results, such as is done for the Ocean Niño Index (ONI) and Cold Tongue Excluded $\delta^{18}O$ SEA as an example in Figure 16. The time series correlate significantly over the 1985-2002 period ($r = 0.805$, non-directional p-value of 0.0002, $N = 16$). Strong ENSO events, particularly the 1987 (La Niña) and 1997 (El Niño), coincide

with significant anomalies in the coral data. This comparison demonstrates the strength of influence that ENSO has on these coral records.

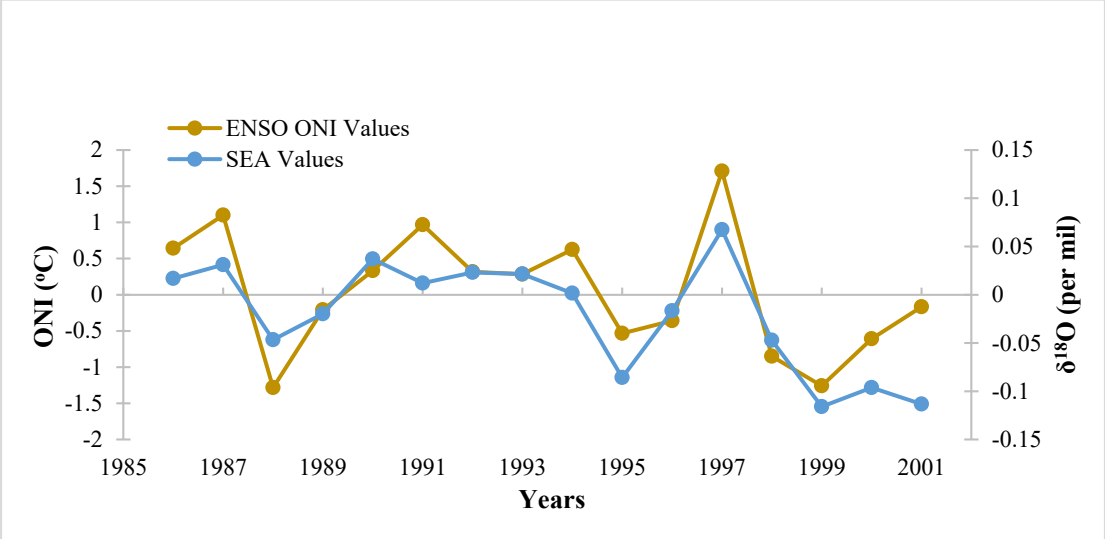

Figure 16. Comparison the ONI (gold) and the $\delta^{18}O$ SEA for the 1991 Mt. Pinatubo when excluding records from the Pacific Cold Tongue (blue). ONI data are from the National Weather Service's Climate Prediction Center and represent the April to March annual average of a 3 month running mean of ERSSTv5 data in the El Niño 3.4 region (Huang et al., 2017). Time series had a r = 0.805, p-value of 0.0002 and N = 16. Two of the major ENSO events (1987 and 1997) in this selected time period coincide with significant anomalies in the coral data.

A contributing factor to a lack of the expected cooling signal after the Pinatubo eruption could be the small GVF of the eruption itself. Any volcanic-induced cooling would have been offset by the ENSO-related warming, possibly explaining why there was such a weak signal associated with the eruption. Better quantification of the instrumental temperature signals from the available study sites would clarify the signal expected in the coral geochemistry data. The approach should be to extract SST time series that match the coral records based on their coordinates and treat them the same way as the coral records were treated in this study. The single event SEA would then be repeated with the SST time series and compared against the SEA performed on the coral records, to serve as a way of

exploring 1) the strength of the signal itself and 2) the ability of the coral in capturing said signal. That also leads us to question, how small is too small of a signal? The relatively small signals obtained from Mt. Pinatubo, for the year of eruption, were not resolvable against the background climate variations, but what about the largest eruption of the last 400 years?

4.2. 1809 "Unknown" and 1815 Mt. Tambora Eruptions

The 1809 and 1815 eruptions produced a GVF of -12.01 W[m^{-2}] and -17.20 W[m^{-2}], respectively (Sigl *et al.,* 2015). In terms of estimated volcanic forcing, these were the third (1809) and first (1815) largest events since the year 1600 C.E. (Sigl *et al.,* 2015). This led to an estimated tropical SST change of −0.53˚C between 1809 and 1810, based on a multi-proxy tropical surface temperature reconstruction, that included primarily tree-ring data but also several corals in this study (D'Arrigo *et al.,* 2009). After the 1815 Tambora eruption, the tropics and extra-tropics experienced a similar cooling of 0.4 – 0.8 ˚C (D'Arrigo *et al.,* 2009, Raible *et al*., 2016). Although my analysis used a relatively small number of available records, the results indicated an even larger temperature decrease, 0.72 ˚C in the year before the eruption, for the 1809 pantropical Sr/Ca SEA, exceeding the background climate variability. Despite Mt. Tambora eruption having the largest GVF, in comparison to that of the 1809 event, its temperature signal was weaker than expected.

A likely explanation for the timing of the strong geochemical anomalies lies in the assignment of years to the geochemical data. As stated in the methods, monthly and bimonthly records were annualized to tropical (April-March) years, with the beginning year (April) chosen as the nominal year for that record. Thus 1809 represents the period of April 1809 to March 1810; months before April 1809 were deemed as belonging to 1808.

There has been some debate in the climate community in terms of the exact timing of this 1809 "Unknown" eruption, with some suggesting it took place in February of 1809 ± 4 months (Cole-Dai *et al.*, 2009), and a recent study of historical documents indicating it likely occurred in late November to December of 1808 (Guevara-Murua *et al.,* 2014). If the eruption took place in late November or beginning of December 1808, the eruption and 4 months afterwards (December-March) would have been categorized as 1808 in this study, potentially explaining the strong cooling present in the SEA(s) during the nominal 1808 year.

Something to consider is the possibility that interannual variability in the climate system, such as ENSO events, may have caused perturbations that are not consistent with the cooling expected after an eruption. Studies have shown that when a volcanic eruption coincides with an ENSO event, one can expect a La Niña (cooling) response the year of the eruption, with an El Niño (warming) response the following year (Stevenson *et al.,* 2017). This could explain why there is warming present the years after the 1809 eruption took place, instead of seeing a cooling period after the eruption. This interannual variability in the climate system could also be responsible for the weak temperature signal produced the year of eruption for Mr. Tambora. 1815 was a known El Niño year (D'Arrigo *et al.,* 2009), which means the temperature signal we are seeing is a combined ENSO + volcanic eruption signal captured in the data, much like in 1991 for the Pinatubo Eruption.

Modeling studies have shown that whether or not an El Niño event is excited by an eruption may be sensitive to the region or hemisphere where an eruption took place (Stevenson *et al.,* 2016). The convolution of ENSO with volcanic forcing likely contributes to discrepancies in the magnitude of the temperature response after an eruption between

modeling and proxy reconstructions studies (McGregor & Timmerman, 2011; Stevenson *et al.,* 2016; Lehner *et al.,* 2016, Dee *et al*. 2020). Much research is needed to understand ENSO's general responses to volcanic events (Stevenson *et al.,* 2016; Stevenson *et al.,* 2017; Otto-Bliesner, 2016).

4.3 All Eruptions

When all substantial eruptions of the last 400 years were composited, a very different signal was detected compared with the single event analyses for the 1991 and early 1800's volcanic events. In this analysis, the strongest signal showed up in the oxygen isotope data, and little in the way of significant signals were detected in the Sr/Ca data. In contrast, the strongest signals came from the Sr/Ca data in the single-event analyses. The oxygen isotopic data showed a distinct cooling/drying response around the year of the eruption, followed by a decadal-scale warming/freshening in the pantropical SEA, which was insensitive to excluding either the Pacific Cold Tongue or the Warm Pool records. A critical difference between this analysis and the single event analyses is that by averaging many events together, the un-forced interannual variability in the record segments (i.e., ENSO) was canceled out, leaving only the volcanic signal. The other analyses focused on particular events, so the resulting SEAs represented the total interannual variability, forced and unforced, over a given period.

Past modeling, instrumental and observational studies have focused on trying to understand the regional responses to strong volcanic eruptions better and how they may influence interannual variability in the climate system (Griesser *et al.,* 1998; Evan *et al.,* 2009; Wang *et al.,* 2017). Each of the regional SEAs done on all nine of the selected eruptions responded differently in terms of temperature and oxygen isotopic changes. The

Pacific Warm Pool had the most robust temperature response to the nine events, whereas the Pacific Cold Tongue and Indian Ocean had a similar reaction but of weaker intensity. This indicates that the Warm Pool might be the center of action of the tropical ocean response to a volcanic event. Although this has not been directly addressed in the scientific literature, research has focused on the effects of strong volcanic eruptions on ENSO events (Adams *et al.,* 2003; Stevenson *et al.,* 2017; Pausata *et al.*, 2015), this finding of a decadal scale response after the eruption(s) warrants further investigation. The Indian Ocean analysis had a large number of records, but a smaller magnitude signal than the Warm Pool. This could indicate a truly weaker signal, or perhaps a mixed eastern and western Indian Ocean Dipole (IOD) signal. The IOD may be excited by volcanic eruptions, as suggested from prior work (Izumo *et al.,* 2018); thus, a stronger signal might be obtained by splitting the Indian Ocean data by the spatial response IOD.

As for the Atlantic Ocean, much of the volcanic eruption research that has been done in this region has focused on the volcanic forcing's effect on Atlantic Multidecadal Variability, AMOC, and how the area itself might play an essential role in its response to the eruptions. Contrary to expectation based on modeling results (Stenchikov *et al.,* 2009, Otto-Bliesner *et al.,* 2016), the Atlantic Ocean's temperature response to the eruptions was virtually non-existent, despite having a similar number of records as the Pacific Warm Pool (~20). This indicates that any volcanic signal in this basin may be too small to be detected relative to the rest of the climatic variability in the region, with the number of records available. One potential source of regional variability in aerosol forcing could be from Saharan dust storms on an interannual basis that are a significant source of temperature variance in the tropical Atlantic (Evan *et al.,* 2009).

In addition to these regional and pantropical responses to the eruptions, these temperature and isotopic changes to the volcanic events indicate decadal-scale warming in the data. Specifically, a decadal-scale warming/freshening was present in the pantropical SEA, and did not change when including/excluding either the Pacific Cold Tongue or Warm Pool records. Past studies have focused on quantifying decadal-to-multidecadal-scale behavior in the tropical oceans in response to strong volcanic eruptions (Stenchikov *et al.,* 2009; Zanchettin *et al.*, 2013). Additionally, research has explored how individual/regional local environmental and background conditions before the eruption could decrease the signal-to-noise ratio in the data for post-eruption decadal and multidecadal-scale climate variability. The global or tropical oceanic temperature response might be easier to interpret. It becomes complicated when looking at the individual/regional background climate conditions that led to that general response (Zanchettin *et al.,* 2013).

The seawater isotopic composition of the coral records in pantropical (as well as including/excluding the Pacific Ocean records), and the regional SEAs, are not only indicative of decadal-scale cooling/freshening years after the eruption but could be directly related to Pacific Decadal Oscillation (PDO; Veettil *et al.* 2014; Vargo, 2013; Wang *et al.* 2012). This aligns with Nurhati *et al*.'s (2011) findings on how seawater oxygen isotopic composition calculated from coral records is directly correlated to PDO. Additional studies have explored how volcanic eruptions, among other types of forcing, influence and play a crucial role in the phasing of the PDO (Wang *et al*., 2012; Smith *et al.,* 2016). Studies conducted coupled atmospheric-oceanic model analyses to better understand the behavior of PDO after strong tropical volcanic eruptions and changes in solar variability. Their

findings indicated that volcanic events could lead to a negative phase of PDO on the climate system (Wang *et al*., 2012; Smith *et al.,* 2016). Past modeling and instrumental studies focused on quantifying this decadal-to-multidecadal behavior in the tropical oceans found that natural volcanic forcing excites multidecadal variability in the Atlantic Ocean (Stenchikov *et al.,* 2009, Otto-Bliesner *et al.,* 2016). This goes against this study's findings as the Pacific Ocean (specifically the Warm Pool) had the more distinct decadal signal, as opposed to the Atlantic Ocean, which had little to no signal 10 to 15 years after the year of the eruption(s). Future work should examine how volcanic eruptions can excite decadal modes of variability in the Pacific, particularly its connections to changes in SST, ocean-atmosphere interactions, and climate forcings (Newman *et al.* 2016).

4.4 Sensitivity Analysis

The data collected for this research provide the opportunity to explore the variability inherent in coral paleoclimate data and the number of records required to obtain a signal of a particular magnitude. Statistically, this is representative of a sensitivity analysis that can determine how detectable effect size changes with sample size, given the variance in these data. The number of data points available for the SEAs in this research varied significantly. The presented analyses demonstrate that when a limited number of data points are available (e.g., for both the 1991 and the 1815 events), a signal must be much larger to exceed the H_0 threshold. In contrast, even small signals exceed the H_0 threshold with bigger sample sizes, such as in the SEA using all available eruptions. Given the combined climate variance and proxy error recorded in coral Sr/Ca and $\delta^{18}O$, how many records are needed to identify a particular climate signal magnitude statistically?

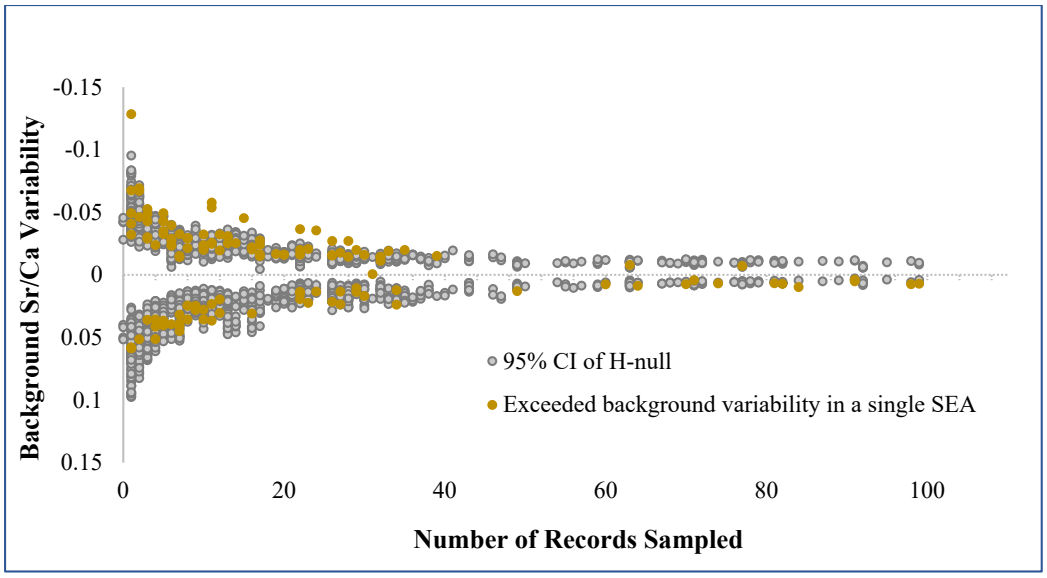

Figure 17. Background climate variability recorded in coral Sr/Ca as a function of the number of records sampled to calculate the background variability. The grey dots represent the positive and negative 95% confidence limits of SEA analyses conducted on randomly selected years from the coral data, after potentially volcanically-influenced data were removed. The grey dots are compiled from the null hypothesis tests described in the methods and shown as yellow bands in each figure displaying an SEA. Data points that exceeded the 95% confidence threshold of any particular analysis are denoted in color.

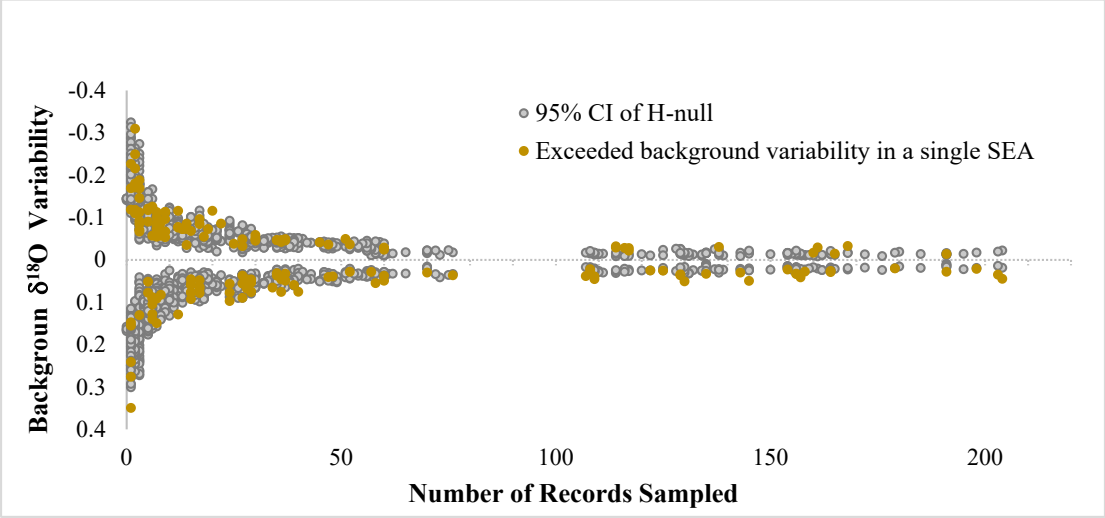

Figure 18. Same as for Figure 14 except for $\delta^{18}O$ data. There is a direct connection between the number of records and the possibility of identifying a signal that surpasses the background variability of the climate system. The higher the number of records the higher the chance of identifying a signal.

To answer how many coral records are needed to resolve a particular geochemical signal from the background variability, I made two scatterplots (Figure 17- 18), one for

Sr/Ca and another for $\delta^{18}O$, to better examine the relationship between the number of records and the obtained 95% CI of H_0 testing. Notably, the 95% CI is a characterization of the data's background variability, composed of the natural climate variability recorded by the corals and any non-climatic variability in the record. By non-climatic variability, I refer to analytical error and environmental error – the sum of different internal and external factors that might influence the way corals record temperature and salinity, such as growth rates and micro-environmental conditions.

For each proxy, I plotted the upper and lower 95% CI's against the number of data points used per year for the SEA's analyzing the Pinatubo, Tambora/Unknown, and all nine eruptions. These figures show that it is difficult to tease out a significant signal from the background noise. The majority of the yellow dots, representing signals that exceeded the background variability in any given analysis, although statistically significant, lie within the cloud of grey dots, within the noise of the data (Figure 17 - 18). If one set a stringent criterion that any detectable volcanic signal (statistical effect level) had to exceed the background variability in any given analysis (the grey cloud), then with ten records, one could resolve a signal of ± 0.035 mmol/mol Sr/Ca (Figure 17) and ± 0.13 ‰ $\delta^{18}O$ (Figure 18). About 40-50 records are needed to detect a smaller signal of approximately ± 0.02 mmol/mol Sr/Ca and approximately ± 0.05 ‰ $\delta^{18}O$. After 50 records, the background variability levels out for both Sr/Ca and $\delta^{18}O$, which means that using more than 50 records does not improve the signal detection from the coral data

It is clear from this work that a high number of data points (40-50 records) are needed to resolve the small volcanic signals from the background climate variability present in the data. ENSO's interannual variability likely contributes to the extensive

background variability relative to volcanic signals' magnitude in these data. Future work should develop novel statistical approaches that increase the signal-to-noise ratio or decrease the records' background variability to better resolve volcanic signals.

Chapter 5: Conclusion

This thesis focused on assessing the temperature and hydroclimate response in the global tropics to the most robust volcanic eruptions of the past 400 years. I used 45 Sr/Ca, and 67 $\delta^{18}O$ coral geochemical records to see if it was possible to capture the volcanic signals and examine if they went above the background climate variability of the records. To explore these areas, I attempted to answer the following questions: (1) How sensitive are coral geochemical records to capturing individual volcanic event signals? Can a climate signal be detected from corals that grew during the relatively small 1991 Mt. Pinatubo eruption? (2) Can we detect the climate impact of a much bigger eruption, with a more limited coral network, for instance, the Mt. Tambora eruption in 1815? (3) Using all coral-based paleoclimate reconstructions available over the last 400 years, is the tropical oceanic temperature and hydroclimate response to strong volcanic eruptions statistically resolvable from the background variability?

To address the previously stated questions, I performed SEAs on two individual (1991 Mt. Pinatubo and 1815 Mt. Tambora) eruptions and nine of the most energetic volcanic eruptions in the past 400 years collectively. SEAs were performed on all Sr/Ca and $\delta^{18}O$ data available that met basic usability criteria. The analyses were conducted on all of the data to create a pantropical SEA as well as from regional subsets of the data. The influence of the Pacific Ocean records on the pantropical SEA was explored by repeating the pantropical analysis with either Pacific Cold Tongue- and Warm Pool-correlated Pacific Ocean records excluded. Regional SEAs were performed for the Atlantic, Indian, Pacific Cold Tongue-correlated and Pacific Warm Pool-correlated regions. To explore the

hydrologic response to the eruptions, I repeated each SEA using paired Sr/Ca and $\delta^{18}O$ records and a calculated the $\delta^{18}Osw$.

The 1991 and 1815 eruptions were used to determine how coral geochemical records capture individual volcanic event signals in terms of oceanic temperature and oxygen isotopic conditions. The 1991 eruption analysis demonstrated that for small eruptions, ENSO variability can overwhelm any forced cooling from volcanic aerosols. This set of SEAs showed the strength of influence that ENSO has on the coral records; some of the most significant temperature and oxygen isotopic anomalies coincided with known ENSO years. On the other hand, the SEAs for Mt. Tambora and the 1809 "Unknown" eruptions demonstrated substantial cooling (high Sr/Ca) associated with the 1809 eruption and a less strong signal associated with the stronger 1815 Tambora eruption. 1815 had a historically documented El Niño event, thus the weaker cooling associated with the Tambora eruption may have been due to a combined volcanic eruption + ENSO forcing as with the 1991 event analysis. Both the 1991 and early 1800's SEAs showed that coral geochemical records could capture volcanic eruptions. Still, the volcanic event's strength might vary due to existing background climatic conditions and variability of the climate system. The background variability could either strengthen or mask volcanic eruption signals in the records, making it a bit difficult to tease out the eruption in the data accurately.

Focusing on the all eruptions SEAs, I used the nine most energetic volcanic eruptions for the past 400 years to determine if the hydroclimate and temperature response was resolvable from the background climate variability of the records. The coral $\delta^{18}O$ data showed a significant increase in the year of the eruption, indicating a decrease in temperature or an increase in seawater oxygen $\delta^{18}O$ or some combination. A similar

magnitude coral $\delta^{18}O$ decrease 10-15 years after the events, indicated a decadal-scale warming and/or seawater $\delta^{18}O$ decrease. Although the signal was found all over the Indo-Pacific (not the Atlantic), the $\delta^{18}O$ increase and decadal-scale decrease was strongest in the Pacific Warm Pool. This signal was resolvable from the background variability only for the $\delta^{18}O$ data; Sr/Ca records had little to no signal detectable for the year of the eruption(s) and for the 10-15 years of decadal variability that was present in the $\delta^{18}O$ coral records.

Lastly, as the number of record segments used varied by SEA, this research provided me with the opportunity to explore the relation between the number of records and the expected size of a geochemical signal. This work showed that 40-50 data points are needed to resolve the small volcanic signals from the background climate variability present in the data.

5.1 Future Directions

Further improvements in sample age assignments could reduce uncertainty in the timing of the climatic response to volcanoes, as recorded in coral geochemistry. In this study, both the early 1800's eruptions, as well as the all eruptions SEAs were indicative of potential age model errors in the data. A possible way to improve age model uncertainty is by focusing on ensuring that the data are annualized in the same way. In this study, sub-seasonal records were annualized by averaging into April to March years and were analyzed along with records that began with an already annual resolution. However, not all annually-resolved data were April-March years. Combining April-March annualized records with yearly resolution records of unknown and potentially variable definitions of a year could impact the signals seen in the resulting SEAs. Future work should focus on

repeating the analyses with data that have a consistent definition of a year to see if it helps with the age uncertainty in the SEAs.

Further, counting errors of 1-2 years per century are not uncommon in coral geochemistry age models. Small age model errors, and their amplitude, in the original coral records could smear or shift signals in the resultant SEA (DeLong *et al.,* 2013; Comboul *et al.,* 2014). These errors are common in coral work and virtually unavoidable, so future work should also minimize the impact of age model uncertainty and test the effects of age model errors on the results. Comboul *et al.,* (2014) attempted to account for age uncertainties by establishing a probabilistic age model for layer-counted records, quantifying their effect on spatiotemporal modes of variability, and adjusting for discrepancies between the cores using an optimization principle based on a general understanding of a multivariate record. Similar approaches could be explored in future analyses.

Future work could also focus on selecting the data by the records' quality in climate signals. Many studies regress coral data to instrumental (local or regional) climate data and either cull by a threshold or weight the records. For example, Tierney *et al.,* (2015) weighted raw non-detrended coral records by their relationship to gridded SST to determine each record's contribution to their composite plus scale (CPS) reconstruction. Another approach that could be taken is that employed by Mann *et al.,* (2008), where they used a screened set of data that passed the threshold of a statistically significant relationship to temperature during the instrumental period. These types of regression methods could be utilized to improve the quality of the records used in the SEA analysis.

The statistical framework of this study leaves room for improvement. Analysis of variance and central tendency assumptions, such as normality, sample independence, and variance equality were explored in the raw unprocessed coral geochemical records but they must be accounted for and tested for in the SEA data instead. If the SEA data are found to satisfy the assumptions, then instead of computing the median SEA, a mean can be used and the standard student-t test for differences in means can be applied as a robust statistical test.

Lastly, some of the chosen eruptions for this study coincided with known ENSO years. One approach to remove the influence of ENSO on the results is to use the El Niño Southern Oscillation Index (SOI) to remove the ENSO signal from the coral records. Robock and Mao (1995) did this in instrumental temperature data by correlating SST anomalies to the SOI, establishing a linear regression, and subsequently removing the ENSO signal. A similar approach could be applied to the coral records in this study.

Making these relatively small changes will greatly improve the study and the scientific impact of future publications based on this work.

Appendix A

Table 2. Coral geochemical records used since 1640 CE.

Ocean	Site Name	Proxy	Start Date	End Date	Reference
Atlantic	Cape Verde	$\delta^{18}O$	1928	2002	Moses *et al.* 2006
Atlantic	Guadeloupe	$\delta^{18}O$	1895	1999	Hetzinger *et al.,* 2010
Atlantic	Los Roques, Venezuela	$\delta^{18}O$	1917	2004	Hetzinger *et al.,* 2008
Atlantic	Bermuda	$\delta^{18}O$	1927	1983	Kuhnert *et al.,* 2005
Atlantic	Biscayne Bay	$\delta^{18}O$	1751	1986	Swart *et al.,* 1996
Atlantic	Florida Bay	$\delta^{18}O$	1824	1985	Swart *et al.,* 1996
Atlantic	Puerto Rico	$\delta^{18}O$	1751	2004	Kilbourne *et al.,* 2008
Atlantic	Bermuda	$\delta^{18}O$	1781	1998	Goodkin *et al.,* 2008
Indian	Abrolhos	$\delta^{18}O$	1794	1993	Kuhnert et al., 1999
Indian	Bali	$\delta^{18}O$	1782	1990	Charles *et al.,* 2003
Indian	Ifaty Tulear	$\delta^{18}O$	1660	1994	Zinke *et al.,* 2014
Indian	Kenya	$\delta^{18}O$	1886	2002	Nakamura *et al.,* 2009
Indian	Mafia Island	$\delta^{18}O$	1896	1998	Damassa *et al.,* 2006
Indian	Mentawai	$\delta^{18}O$	1858	1997	Abram *et al.,* 2008
Indian	Ningaloo	$\delta^{18}O$	1879	1995	Kuhnert *et al*., 2000
Indian	Ras Umm Sid, Red Sea	$\delta^{18}O$	1751	1995	Felis *et al*., 2000
Indian	La Reunion	$\delta^{18}O$	1832	1995	Pfeiffer *et al*., 2004
Indian	Ras Um Sid, Red Sea	$\delta^{18}O$	1897	1993	Moustafa, 2000
Indian	Seychelles	$\delta^{18}O$	1846	1995	Charles *et al*., 1997
Indian	Mayotte	$\delta^{18}O$	1881	1994	Zinke *et al.,* [2008, 2009]

Indian	Cocos DL	$\delta^{18}O$	1808.17	2009	Hennekam *et al.,* 2018
Indian	Madagascar	$\delta^{18}O$	1659	1995	Zinke *et al*., 2004
Indian	Abrolhos	$\delta^{18}O$	1795	2010	Zinke *et al*., 2014
Indian	Aqaba	$\delta^{18}O$	1788	1992	Heiss *et al*., 1994
Indian	Aqaba	$\delta^{18}O$	1886	1992	Heiss *et al*., 1994
Indian	Tulear	$\delta^{18}O$	1882	1994	Zinke *et al*., 2014
Indian	Tulear	$\delta^{18}O$	1905	1994	Zinke *et al*., 2014
Indian	Malindi	$\delta^{18}O$	1801	1994	Cole *et al*., 2000
Indian	Cocos D3	$\delta^{18}O$	1808.17	2009.58	Hennekam *et al*., 2018
Pacific	Bunaken	$\delta^{18}O$	1860	1990	Charles *et al*., 2003
Pacific	Gorman	$\delta^{18}O$	1842.63	2007.63	Gorman *et al*., 2012
Pacific	Guam	$\delta^{18}O$	1790	2000	Asami *et al*., 2005
Pacific	Liang	$\delta^{18}O$	1884	1993	Tudhope *et al*., 2001
Pacific	Rarotonga	$\delta^{18}O$	1726.78	1996.91	Linsley *et al.,* 2006
Pacific	Rarotonga	$\delta^{18}O$	1874.68	2000.18	Linsley *et al.,* 2006
Pacific	Rarotonga	$\delta^{18}O$	1906.88	1999.75	Linsley *et al.,* 2006
Pacific	Madang	$\delta^{18}O$	1880.79	1993.04	Tudhope *et al.,* 2001
Pacific	Palau Rocki Islands	$\delta^{18}O$	1899.17	2008.17	Osborne *et al*., 2014
Pacific	Palau Ulong Channel	$\delta^{18}O$	1793.17	2008.17	Osborne *et al.,* 2014
Pacific	Papua New Guinea	$\delta^{18}O$	1922.54	1991.29	Tudhope *et al*., 1995
Pacific	Rabaul	$\delta^{18}O$	1867.38	1997.54	Quinn *et al.,* 2006
Pacific	Espiritu Santo, Vanuatu	$\delta^{18}O$	1928	1992	Kilbourne *et al*., 2004
Pacific	Misima, Papua New Guinea	$\delta^{18}O$	1555	1644	Hereid *et al.,* 2013

Pacific	Espiritu Santo, Vanuatu	$\delta^{18}O$	1807	1979	Quinn *et al.,* 1996
Pacific	Clipperton	$\delta^{18}O$	1874.08	1956.79	Wu *et al*., 2014
Pacific	Clipperton	$\delta^{18}O$	1893.79	1994.04	Linsley *et al.,* 2000
Pacific	Ogasawara, Japan	$\delta^{18}O$	1873	1993	Felis *et al.,* 2009
Pacific	Kiritimati	$\delta^{18}O$	1938.29	1993.63	Evans *et al.,* 1998
Pacific	Maiana	$\delta^{18}O$	1840	1994	Urban *et al*., 2000
Pacific	Nauru	$\delta^{18}O$	1898	1995	Guilderson *et al*., 1999
Pacific	Palmyra	$\delta^{18}O$	928	1998	Cobb *et al*., 2003
Pacific	Secas Island, Panama	$\delta^{18}O$	1707	1984	Linsley *et al*., 1994
Pacific	Palmyra	$\delta^{18}O$	1886.13	1998.29	Nurhati *et al.,* 2011
Pacific	Kupang Bay, Timor, Indonesia	$\delta^{18}O$	1914	2004	Cahyarini *et al*., 2014
Pacific	Urvina Bay, Galapagos Islands	$\delta^{18}O$	1607	1981	Dunbar *et al*., 1994
Pacific	Great Barrier Reef	$\delta^{18}O$	1635	1991	Druffel *et al.,* 1999
Pacific	Savusavu Bay, Fiji	$\delta^{18}O$	1781	1997	Linsley *et al.,* 2006
Pacific	Savusavu Bay, Fiji	$\delta^{18}O$	1617	2001	Linsley *et al.,* 2006
Pacific	Moorea Lagoon, French Polynesia	$\delta^{18}O$	1852	1990	Boiseau *et al., 1999*
Pacific	Savusavu Bay, Fiji	$\delta^{18}O$	1776	2001	Bagnato *et al*., 2005
Pacific	Christmas Island	$\delta^{18}O$	1972.13	1998.38	Nurhati *et al.,* 2009
Pacific	Fanning	$\delta^{18}O$	1972.13	2005.54	Nurhati *et al.,* 2009
Pacific	Hon Tre Island, Vietnam	$\delta^{18}O$	1977	2010	Bolton *et al*., 2014
Pacific	Kiribati	$\delta^{18}O$	1959	2010	Carilli *et al.,* 2014
Pacific	Palaui Islands, Philippines	$\delta^{18}O$	1962	2012	Ramos *et al.,* 2017
Pacific	Palaui	$\delta^{18}O$	1954	2012	Ramos *et al.,* 2017

Atlantic	Dry Tortugas	Sr/Ca	1733.79	2008.63	DeLong *et al*., 2014
Atlantic	Guadeloupe	Sr/Ca	1895	1998	Hetzinger *et al*., 2010
Atlantic	Bermuda	Sr/Ca	1927	1983	Kuhnert *et al.,* 2005
Atlantic	Puerto Rico	Sr/Ca	1751	2004	Kilbourne *et al.,* 2008
Atlantic	Bermuda	Sr/Ca	1781	1998	Goodkin *et al*., 2008
Atlantic	Anegada	Sr/Ca	1990.12	2008.13	Xu *et al.,* 2015
Indian	Mayotte	Sr/Ca	1881	1994	Zinke *et al.,* [2008, 2009]
Indian	Cocos Island	Sr/Ca	1808	2009	Hennekam *et al.,* 2018
Indian	Rodrigues Island	Sr/Ca	1945	2006	Zinke *et al*., 2016
Indian	Rodrigues Island	Sr/Ca	1781	2005	Zinke *et al*., 2016
Indian	Imperieuse	Sr/Ca	1806	2009	Zinke *et al.,* 2015
Indian	Imperieuse	Sr/Ca	1798	2009	Zinke *et al.,* 2015
Indian	Mermaid	Sr/Ca	1891	2009	Zinke *et al.,* 2015
Indian	Tantabiddi	Sr/Ca	1952	1999	Zinke *et al.,* 2015
Indian	Madagaskar-Ifaty Reef	Sr/Ca	1659	1995	Zinke *et al.,* 2004
Indian	Abrohos	Sr/Ca	1798	2010	Zinke *et al.,* 2014
Indian	Cocos Island	Sr/Ca	1987	2009	Hennekam *et al.,* 2018
Indian	Abrohos	Sr/Ca	1847	2010	Zinke *et al.,* 2014
Indian	Bundegi, Ningaloo Reef	Sr/Ca	1961	2008	Zinke *et al*., 2015
Indian	Clerke Reef	Sr/Ca	1891	2009	Zinke *et al.,* 2015
Pacific	Kavieng, Papua New Guinea	Sr/Ca	1823	1997	Alibert *et al.,* 2008
Pacific	Rarotonga	Sr/Ca	1726	1996	Linsley *et al*., 2006
Pacific	New Caledonia	Sr/Ca	1649	1999	Delong *et al*., 2012

Pacific	Rabaul	Sr/Ca	1867.38	1997.54	Quinn *et al*., 2006
Pacific	Vanuatu	Sr/Ca	1928	1992	Kilbourne *et al*., 2004
Pacific	Misima	Sr/Ca	1644	1555	Hereid *et al.,* 2013
Pacific	Tonga	Sr/Ca	1791	2003	Wu *et al.,* 2013
Pacific	Clipperton	Sr/Ca	1934.88	1993.96	Wu *et al.,* 2014
Pacific	Clipperton	Sr/Ca	1894.04	1993.96	Wu *et al.,* 2014
Pacific	Clipperton	Sr/Ca	1941.96	1993.96	Wu *et al.,* 2014
Pacific	Clipperton	Sr/Ca	1874.08	1956.79	Wu *et al.,* 2014
Pacific	Ogasawara, Japan	Sr/Ca	1873	1993	Felis *et al*., 2009
Pacific	Sansha Island, Xisha Islands, South China Sea	Sr/Ca	1906	1994	Sun *et al.,* 2004
Pacific	Palmyra Island	Sr/Ca	1886	1998	Nurhati *et al.,* 2011
Pacific	Kupang Bay, Timor, Indonesia	Sr/Ca	1914	2004	Cahyarini *et al*., 2014
Pacific	Galapagos	Sr/Ca	1940	2010	Jimenez *et al*., 2018
Pacific	Savusavu Bay, Fiji	Sr/Ca	1781	1997	Linsley *et al.,* 2006
Pacific	Christmas Island	Sr/Ca	1972	1998	Nurhati *et al*., 2009
Pacific	Fanning	Sr/Ca	1972	2005	Nurhati *et al*., 2009
Pacific	Galapagos	Sr/Ca	1940	2010	Jimenez *et al.,* 2018
Pacific	Keppel Island	Sr/Ca	1958	2010	Saha *et al*., 2017
Pacific	Hon Tren Island	Sr/Ca	1977	2010	Bolton *et al.,* 2014
Pacific	Butaritari Atoll, Kiribati	Sr/Ca	1959	2010	Carilli *et al.,* 2014
Pacific	Palaui	Sr/Ca	1954	2012	Ramos *et al*., 2017
Pacific	Palaui	Sr/Ca	1954	2012	Ramos *et al*., 2017

Appendix B. SEA: 1991 Mt. Pinatubo

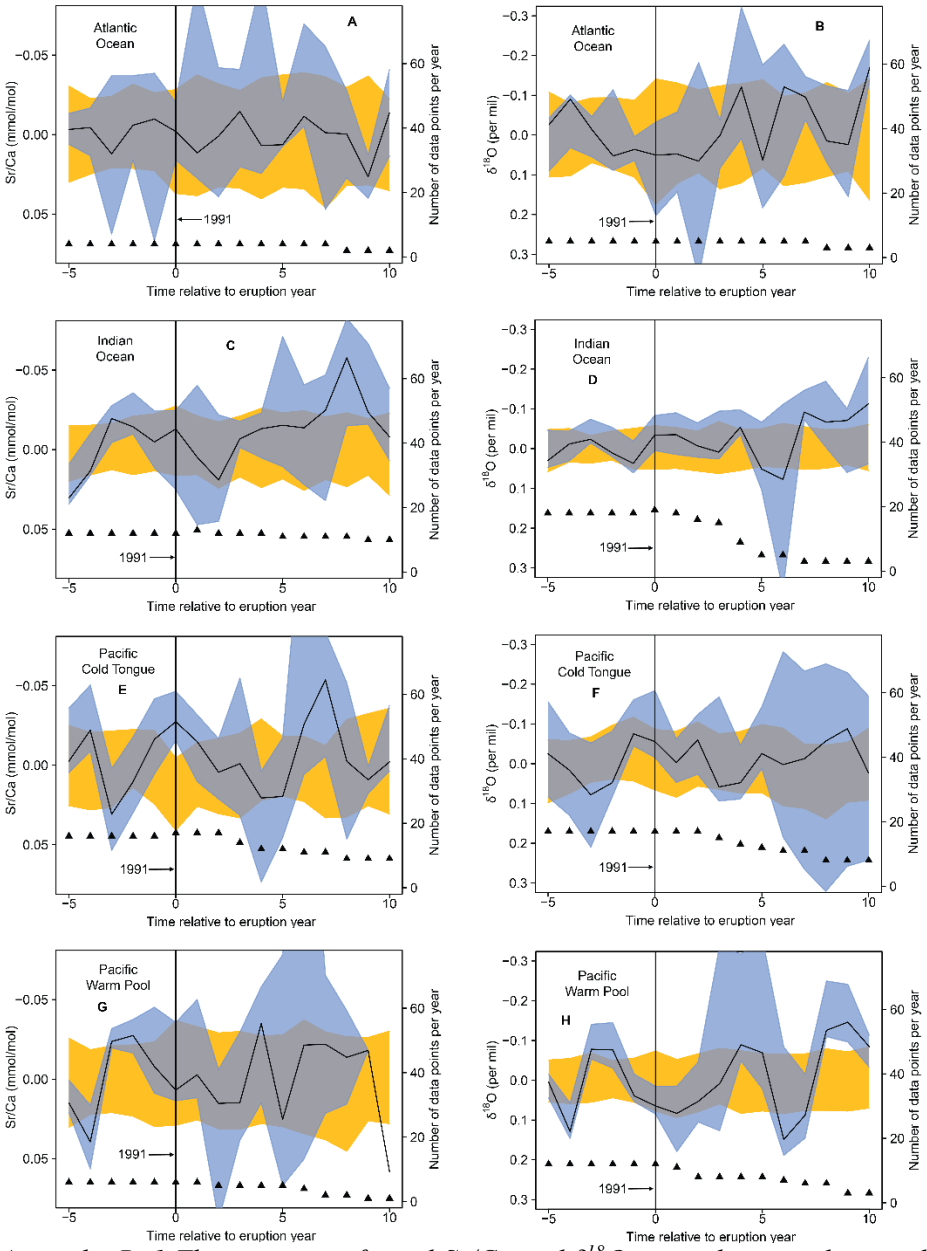

Appendix B. 1 The response of coral Sr/Ca and $\delta^{18}O$, in each tropical ocean basin, to the 1991 Mt. Pinatubo volcanic eruption using all coral records available. The Warm Pool and Cold Tongue from the Pacific Ocean represent the records as they were correlated to ENSO, not the geographical ranges. The black line is the median response to the volcanic eruptions and the blue shaded area represents its 95% CI. The yellow shaded area represents the 95% CI for 100 SEA calculations using randomly selected non-eruption years from the same records. Vertical line at year zero represents the year of eruption, while the black triangles represent the number of coral records available for each year (right-axis). Possible warming at year zero for Sr/Ca in the Pacific Cold Tongue.

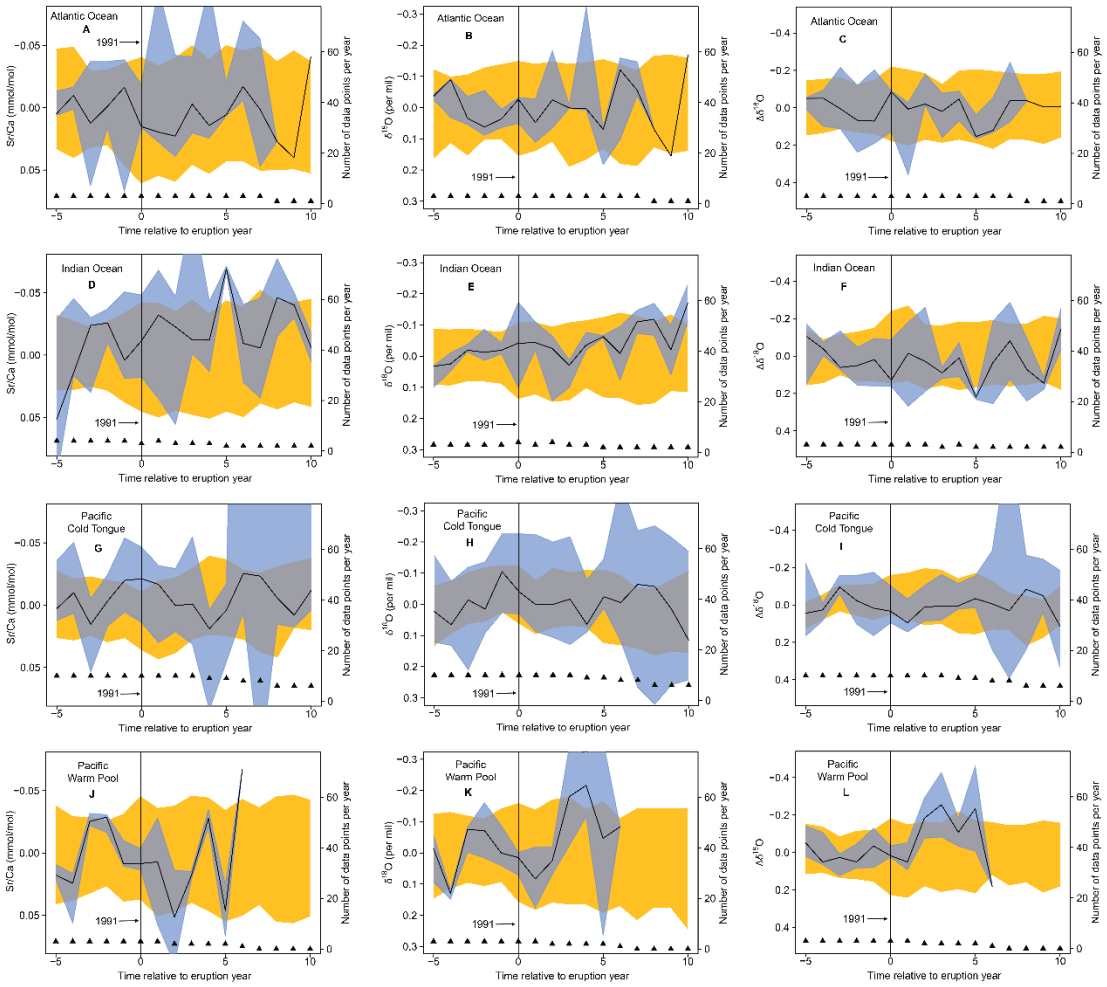

Appendix B. 2. The response of coral Sr/Ca, $\delta^{18}O$ and $\Delta\delta^{18}O$, in each tropical ocean basin, to the 1991 Mt. Pinatubo volcanic eruption using all paired coral records available. The Warm Pool and Cold Tongue from the Pacific Ocean represent the records as they were correlated to ENSO, not the geographical ranges. The figure descriptions are the same as in Appendix B.1.. Lack of data points in the years following the eruption led to an increase in the variance of the yellow band; this does not represent the true uncertainty of the results.

Appendix C. SEA: 1809 'Unknown' and 1815 Tambora Eruptions

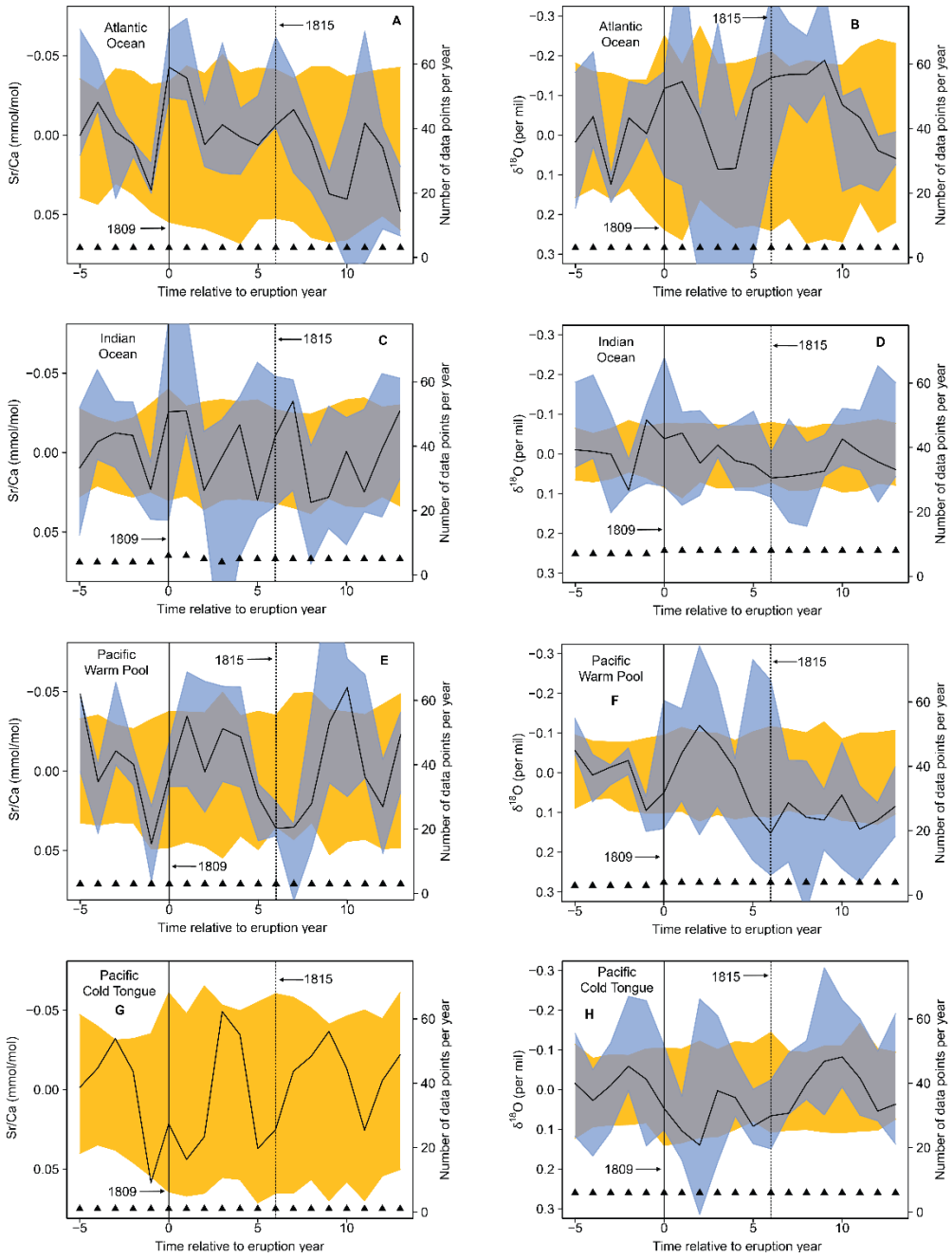

Appendix C. 1 The response of coral Sr/Ca and $\delta^{18}O$ in each tropical ocean basin to the 1809 "Unknown" and 1815 Mt. Tambora eruptions using all coral records available. The Warm Pool and Cold Tongue from the Pacific Ocean represent the records as they were correlated to ENSO, not the geographical ranges. The figure descriptions are the same as in Appendix B.1. Lack of individual records per region to calculate the 95% CI to the median response to both eruptions.

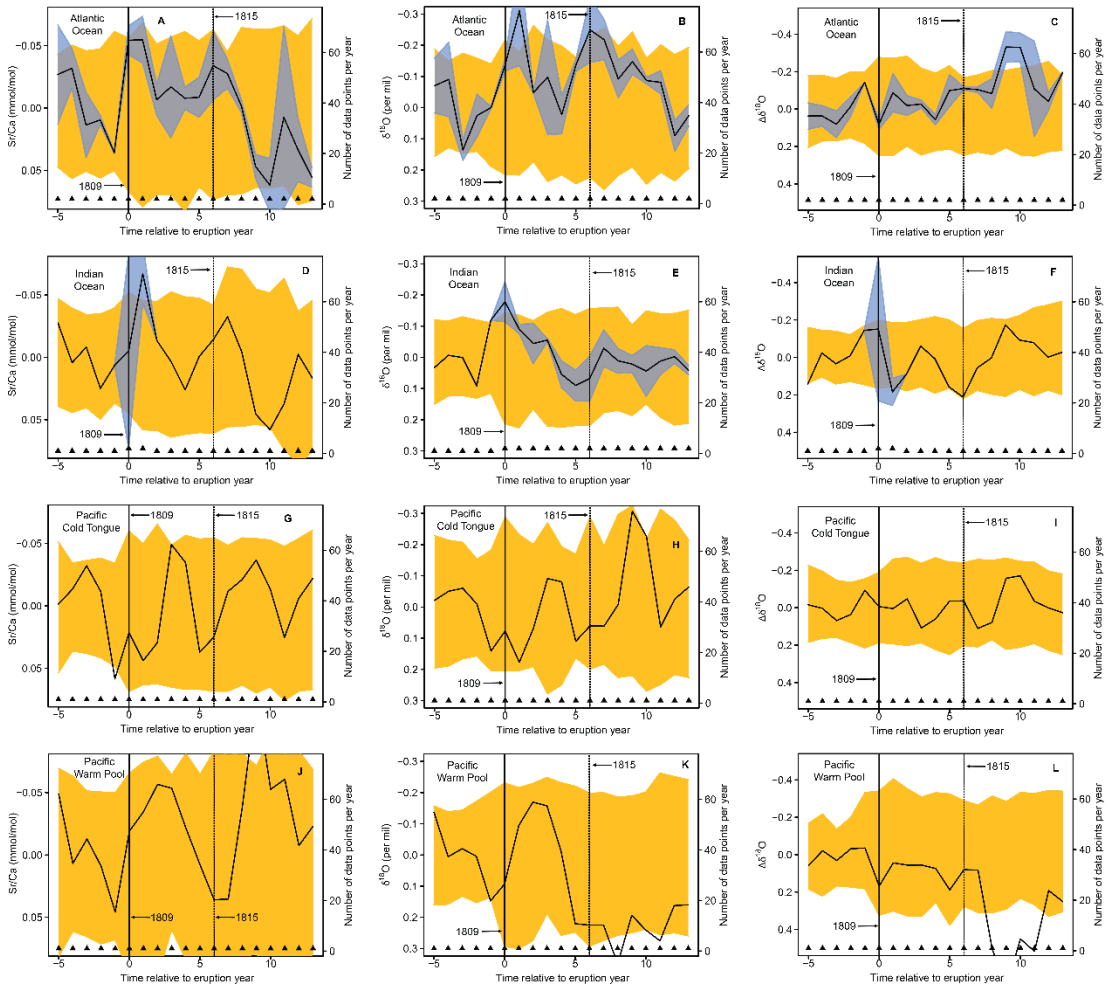

Appendix C. 2 The response of coral Sr/Ca, $\delta^{18}O$ and $\Delta\delta^{18}O$ in each tropical ocean basin to the 1809 "Unknown" and 1815 Mt. Tambora eruptions using all paired coral records available. The Warm Pool and Cold Tongue from the Pacific Ocean represent the records as they were correlated to ENSO, not the geographical ranges. Figure description is the same as in Appendix B.1. There is lack of individual records per region to calculate the 95% CI to the median response to both eruptions.

Appendix D. SEA: All Eruptions

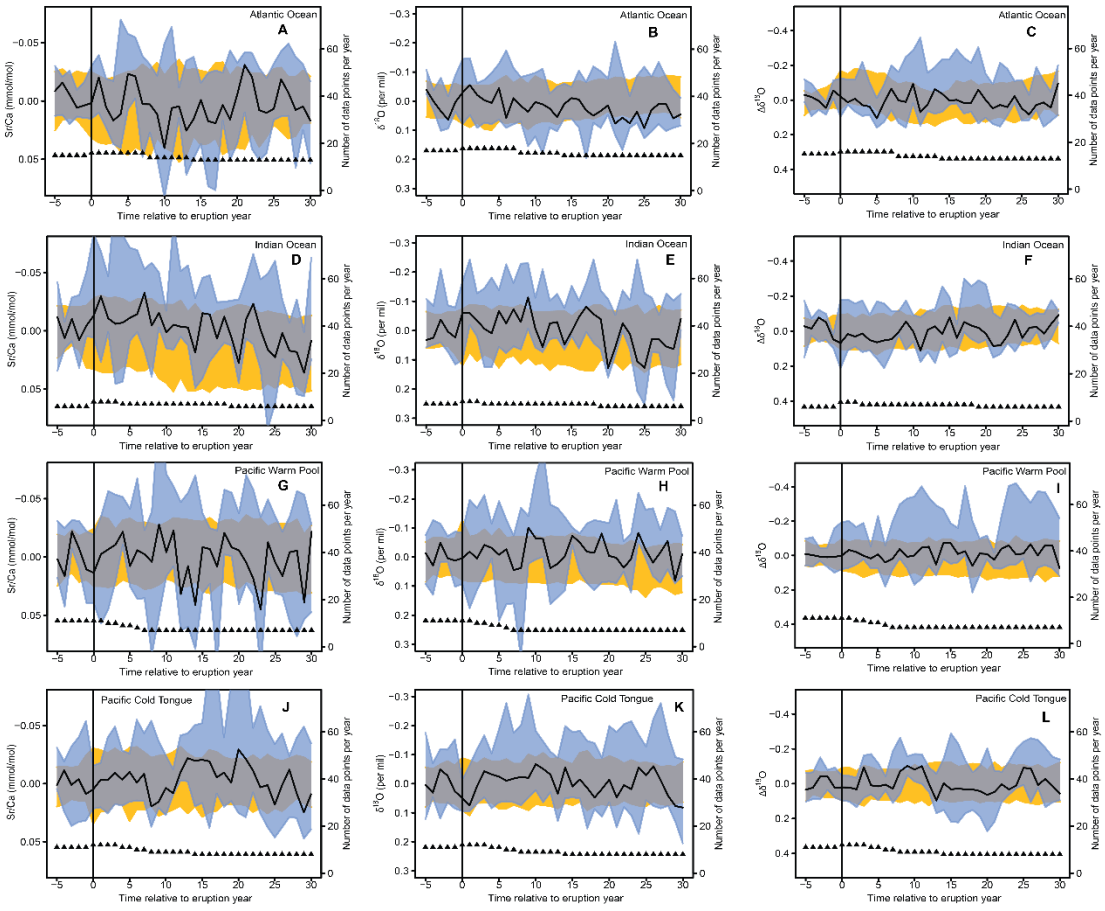

Appendix D. 1. The response of coral Sr/Ca, $\delta^{18}O$ and $\Delta\delta^{18}O$ in each tropical ocean basin to all nine eruptions using all paired coral records available. Figure description is the same as in Appendix B.1. No significant signal was detected that surpassed the 95% CI of null hypothesis testing.

Bibliography

Abram, N. J., McGregor, H. V., Tierney, J. E., Evans, M. N., McKay, N. P., Darrell, S. K., & PAGES 2k Consortium. (2016). Early onset of industrial-era warming across the oceans and continents. *536*(411). https://doi.org/doi:10.1038/nature19082

Abram, N.J., M.K. Gagan, J.E. Cole, W.S. Hantoro, and Mudelsee, M. (2008). Recent intensification of tropical climate variability in the Indian Ocean. Nature Geoscience, 1 (12), 849-853. doi:10.1038/ngeo357.

Adams, J. B., Mann, M. E., and Ammann, C. M. (2003). Proxy evidence for an El Niño-like response to volcanic forcing. *Nature*, *426*(6964), 274–278. https://doi.org/10.1038/nature02101

Alibert, C., & McCulloch, M. T. (1997). Strontium/calcium ratios in modern *porites* corals from the Great Barrier Reef as a proxy for sea surface temperature: Calibration of the thermometer and monitoring of ENSO. *Paleoceanography*, *12*(3), 345–363. https://doi.org/10.1029/97PA00318

Alibert, C., and Kinsley, L. (2008). A 170-year Sr/Ca and Ba/Ca coral record from the western Pacific warm pool: 2. A window into variability of the New Ireland Coastal Undercurrent. J. Geophys. Res., 113, C06006.

Ammann, C. M., Meehl, G. A., Washington, W. M., and Zender, C. S. (2003). A monthly and latitudinally varying volcanic forcing dataset in simulations of 20th century climate: Volcanic Forcing Dataset of 20th Century. *Geophysical Research Letters*, *30*(12). https://doi.org/10.1029/2003GL016875

Asami, R.,Yamada, T., Iryu, Y., Quinn, T.M., Meyer, C.P., and Paulay, G. (2005). Interannual and decadal variability of the western Pacific sea surface condition for

the years 1787-2000. Journal of Geophysical Research: Oceans, 110. doi: 10.1029/2004JC002555

Bagnato, Stefan., Linsley, Braddock K., Howe, Stephen S., Wellington, Gerard M., Salinger, Jim. (2005). Coral oxygen isotope records of interdecadal climate variations in the South Pacific Convergence Zone region. Geochemistry, Geophysics, Geosystems, 6(6), Q06001. doi: 10.1029/2004gc000879

Berk, R. A. (2016). Statistical Learning from a Regression Perspective. *Springer Texts in Statistics, Springer, Switzerland*, *2nd Edition*. https://doi.org/10.1007/ 978-3-319-44048-4

Blake, S., Lewis, S. C., and LeGrande, A. N. (2017). Assessing the impact of large volcanic eruptions of the Last Millennium on Australian rainfall regimes. Feedback and Forcing/Modelling only/Decadal-Seasonal. https://doi.org/10.5194/cp-2017-109

Boiseau, M., Ghil, M., and Juillet-Leclerc, A. (1999). Climatic trends and interdecadal variability from South-Central Pacific coral records. Geophysical Research Letters, 26.

Bolton, A., Goodkin, N. F., Hughen, k., Ostermann, D. R., Vo, S. T., and Phan, H. K. (2014). Paired Porites coral Sr/Ca and $\delta^{18}O$ from the western South China Sea: Proxy calibration of sea surface temperature and precipitation. *410*. https://doi.org/10.1016/j.palaeo.2014.05.047

Bradley, R. S. (1988). The Explosive Volcanic Eruption Signal in the Northern Hemisphere Continental Temperature Records. *Climatic Change*, *12*, 221–243. https://doi.org/10.1007/BF00139431

Cahyarini, S. Y., Pfeiffer, M., Timm, O., Dullo, W.-C., and Schönberg, D. G. (2008). Reconstructing seawater $\delta^{18}O$ from paired coral $\delta^{18}O$ and Sr/Ca ratios: Methods, error analysis and problems, with examples from Tahiti (French Polynesia) and Timor (Indonesia). *Geochimica et Cosmochimica Acta*, *72*(12), 2841–2853. https://doi.org/10.1016/j.gca.2008.04.005

Cahyarini, S.Y., M. Pfeiffer, I.S. Nurhati, E. Aldrian, W.-C. Dullo, and S. Hetzinger. (2014). Twentieth century sea surface temperature and salinity variations at Timor inferred from paired coral d18O and Sr/Ca measurements. Journal of Geophysical Research: Oceans, 119, 4593–4604. doi: 10.1002/2013JC009594

Carilli, J.E., H.V. McGregor, J.J. Gaudry, S.D. Donner, M.K. Gagan, S. Stevenson, H. Wong, and D. Fink. (2014). Equatorial Pacific coral geochemical records show recent weakening of the Walker Circulation. Paleoceanography. doi: 10.1002/2014PA002683

Charles, C.D., Hunter, D.E., and Fairbanks, R.G. (1997). Interaction between the ENSO and the Asian monsoon in a coral record of tropical climate. Science, 277, 925-928.

Charles, Christopher D., Cobb, Kim., Moore, Michael D., and Fairbanks, Richard G. (2003). Monsoon-tropical ocean interaction in a network of coral records spanning the 20th century. Marine Geology, 201(1-3), 207-222. doi: 10.1016/S0025-3227(03)00217-2

Chen, K., Ning, L., Liu, Z., Liu, J., Sun, W., Yan, M., Liu, B., Qin, Y., and Xue, J. (2020). The Influences of Tropical Volcanic Eruptions with Different Magnitudes on Persistent Droughts over Eastern China. *Atmosphere*, *11*(2), 210. https://doi.org/10.3390/atmos11020210

Cobb, K., Charles, C., Cheng, H., Edwards, L. (2003). El Niño/Southern Oscillation and tropical Pacific climate during the last millennium. Nature, 424, 271-276. doi: 10.1038/nature01779

Cole, J.E., Dunbar, R.B., McClanahan, T.R., and Muthiga, N. (2000). Tropical Pacific forcing of decadal variability in the western Indian Ocean over the past two centuries. Science, 287(5453). doi: 10.1126/science.287.5453.617

Cole-Dai, J., Ferris, D., Lanciki, A., Savarino, J., Baroni, M., and Thiemens, M. H. (2009). Cold decade (AD 1810–1819) caused by Tambora (1815) and another (1809) stratospheric volcanic eruption, *36*(L22703), https://doi.org/10.1029/2009GL040882

Comboul, M., Emile-Geay, J., Evans, M. N., Mirnateghi, N., Cobb, K. M., and Thompson, D. M. (2014). A probabilistic model of chronological errors in layer-counted climate proxies: applications to annually banded coral archives. Clim. Past, 10, 825–841, 2014 www.clim-past.net/10/825/2014/ doi:10.5194/cp-10-825-2014.

Corrège, Thierry. (2006). Sea surface temperature and salinity reconstruction from coral geochemical tracers. ELSEVIER. Palaeogeography, Palaeoclimatology, Palaeoecology 232 (2006), 408 – 428. doi:10.1016/j.palaeo.2005.10.014

Crowley, T. J., and Unterman, M. B. (2013). Technical details concerning development of a 1200 yr proxy index for global volcanism. *Earth System Science Data*, *5*(1), 187–197. https://doi.org/10.5194/essd- 5-187-2013

Crowley, Thomas J., Quinn, T. M., Taylor, F. W., Henin, C., & Joannot, P. (1997). Evidence for a volcanic cooling signal in a 335-year coral record from New

Caledonia. *Paleoceanography*, *12*(5), 633–639. https://doi.org/10.1029/97PA01348

D'Arrigo, R., Wilson, R., and Anchukaitis, K. J. (2013). Volcanic cooling signal in tree ring temperature records for the past millennium: Volcanism and Tree Ring Records. *Journal of Geophysical Research: Atmospheres*, *118*(16), 9000–9010. https://doi.org/10.1002/jgrd.50692

D'Arrigo, R., Wilson, R., and Tudhope, A. (2009). The impact of volcanic forcing on tropical temperatures during the past four centuries. *Nature Geoscience*, *2*(1), 51–56. https://doi.org/10.1038/ngeo393

D'Arrigo, R., Wilson, R., Liepert, B., and Cherubini, P. (2008). On the 'Divergence Problem' in Northern Forests: A review of the tree-ring evidence and possible causes. *Global and Planetary Change*, *60*(3–4), 289–305. https://doi.org/10.1016/j.gloplacha.2007.03.004

DallaSanta, K., Gerber, E. P., and Toohey, M. (2019). The Circulation Response to Volcanic Eruptions: The Key Roles of Stratospheric Warming and Eddy Interactions. *Journal of Climate*, *32*(4), 1101–1120. https://doi.org/10.1175/JCLI-D-18-0099.1

Damassa, T.D., Cole, J.E., Barnett, H.R., Ault, T.R. and McClanahan, T.R. (2006). Enhanced multidecadal climate variability in the 17th century from coral isotope records in the western Indian Ocean. Paleoceanography, 21, PA2016, doi: 10.1029/2005PA001217

Dee, S. G., Cobb, K. M., Emile-Geay, J., Ault, T. R., Edwards, R. L., Cheng, H., and Charles, C. D. (2020). No consistent ENSO response to volcanic forcing over the last millennium. *Science*, *367*(6485), 1477–1481.

https://doi.org/10.1126/science.aax2000

DeLong, K.L., J. Flannery, R.Z. Poore, T.M. Quinn, C.R. Maupin, K. Lin, and C.-C. Shen. (2014). A reconstruction of sea surface temperature variability in the southeastern Gulf of Mexico from 1734-2008 CE using cross-dated Sr/Ca records from the coral Siderastrea siderea. Paleoceanography. . doi: 10.1002/2013PA002524

DeLong, Kristine L., Quinn, Terrence M., Taylor, Frederick W., Shen, Chuan-Chou.., and Lin, Ke.(2013).Improving coral-base paleoclimate reconstructions by replicating 350 years of coral Sr/Ca variation. Elsevier, 373, 6-24. https://doi.org/10.1016/j.palaeo.2012.08.019

DeLong, Kristine L., Quinn, Terrence M., Taylor, Frederick W., Lin, Ke., and Shen, Chuan-Chou. (2012). Sea surface temperature variability in the southwest tropical Pacific since AD 1649. Nature Climate Change, 2, 799-804. doi: 10.1038/nclimate1583

Druffel, E.R.M., and Griffin, S. (1999). Variability of surface ocean radiocarbon and stable isotopes in the southwestern Pacific. Journal of Geophysical Research: Oceans, 104.

Dunbar, R.B., Wellington, G.M., Colgan, M.W., and Glynn, P.W. (1994). Eastern Pacific sea surface temperature since 1600 A.D.: The $\delta^{18}O$ record of climate variability in Galapagos corals. Paleoceanography 9:291-315.

Esptein, S., Buchsbaum, R., Lowenstam, H. A., and Urey, H. C. (1953). Revised Carbonate-Water Isotopic Temperature Scale. *64*(11), 1315–1326. https://doi.org/10.1130/0016-7606

Evan, A. T., Vimont, D. J., Heidinger, A. K., Kossin, J. P., and Bennartz, R. (2009). The Role of Aerosols in the Evolution of Tropical North Atlantic Ocean Temperature Anomalies. *Science*, *324*(5928), 778–781. https://doi.org/10.1126/science.1167404

Evans, M.N., Fairbanks, R.G., and Rubenstone, J.L. (1998). A Proxy Index of ENSO Teleconnections. Nature, 394.

Fairbanks, R. G., Evans, M. N., Rubenstone, J. L., Mortlock, R. A., Broad, K., Moore, M. D., and Charles, C.D. (1997). Evaluating climate indices and their geochemical proxies measured in corals. *Coral Reefs*, *16*(5), S93–S100. https://doi.org/10.1007/s003380050245

Felis, T., Suzuki, A., Kuhnert, H., Dima, M., Lohmann, G., and Kawahata, H. (2009). Subtropical coral reveals abrupt early-twentieth-century freshening in the western North Pacific Ocean. Geology, 37(6), 527-530. doi:10.1130/G25581A.1

Felis, Thomas., Pätzold, Jürgen., Loya, Yossi., Fine, Maoz., Nawar, Ahmed H., and Wefer, Gerold. (2000). A coral oxygen isotope record from the northern Red Sea documenting NAO, ENSO, and North Pacific teleconnections on Middle East climate variability since the year 1750. Paleoceanography, 15(6), 679-694. doi: 10.1029/1999PA000477

Fischer, E. M., Luterbacher, J., Zorita, E., Tett, S. F. B., Casty, C., and Wanner, H. (2007). European climate response to tropical volcanic eruptions over the last half millennium: Climate Response to Volcanic Eruptions. *Geophysical Research Letters*, *34*(5), https://doi.org/10.1029/2006GL027992

Flannery, Jennifer A., Richey, Julie N., Thirumalai, Kaustubh., Poore, Richard Z., and DeLong, Kristine L. (2017). Multi-species coral Sr/Ca-based sea-surface

temperature reconstruction using Orbicella faveolata and Siderastrea siderea from the Florida Straits. ELSEVIER. Palaeogeography, Palaeoclimatology, Palaeoecology. Volume 466, 100-109 doi.org/10.1016/j.palaeo.2016.10.022

Gagan, M. K. (1998). Temperature and Surface-Ocean Water Balance of the Mid-Holocene Tropical Western Pacific. *Science*, *279*(5353), 1014–1018. https://doi.org/10.1126/science.279.5353.1014

Gagan, Michael K., Dunbar, G. B., and Suzuki, A. (2012). The effect of skeletal mass accumulation in *Porites* on coral Sr/Ca and δ^{18}O Paleothermometry: Skeletogenesis and Coral Thermometry. *Paleoceanography*, *27*(1). https://doi.org/10.1029/2011PA002215

Gao, C., Gao, Y., Zhang, Q., and Shi, C. (2017). Climatic aftermath of the 1815 Tambora eruption in China. *Journal of Meteorological Research*, *31*(1), 28–38. https://doi.org/10.1007/s13351-017-6091-9 Gao, C.,

Gao, Chaochao., Robock, Alan., and Ammann, Caspar. (2008). Volcanic forcing of climate over the past 1500 years: An improved ice core-based index for climate models. Journal of Geophysical Research, 113(D23111). doi:10.1029/2008JD010239.

Garrison, C. S., Kilburn, C. R. J., and Edwards, S. J. (2018). The 1831 eruption of Babuyan Claro that never happened: Has the source of one of the largest volcanic climate forcing events of the nineteenth century been misattributed? *Journal of Applied Volcanology*, *7*(1), 8. https://doi.org/10.1186/s13617-018-0078-9

Gillett, N. P., Weaver, A. J., Zwiers, F. W., and Wehner, M. F. (2004). Detection of volcanic influence on global precipitation: Volcanic Influence on Precipitation.

Geophysical Research Letters, *31*(12), https://doi.org/10.1029/2004GL020044

Goodkin, N.F., Hughen, K.A., Curry, W.B., Doney, S.C. and Ostermann, D.R. (2008). Sea surface temperature and salinity variability at Bermuda during the end of the Little Ice Age. Paleoceanography, 23(PA3203).

Gorman, M.K., Quinn, T.M., Taylor, F.W., Partin, J.W., Cabioch, G., Austin Jr., J.A., Pelletier, B., Ballu, V., Maes, C., and Saustrup, S. (2012). A coral-based reconstruction of sea surface salinity at Sabine Bank, Vanuatu from 1842 to 2007 CE. Paleoceanography, 27(PA3226). doi: 10.1029/2012PA002302

Grieser, J., and Schonwiese, C.-D. (1998). Parameterization of spatio-temporal patterns of volcanic aerosol induced stratospheric optical depth and its climate radiative forcing. 23.

Gu, G., and Adler, R. F. (2010). Precipitation and Temperature Variations on the Interannual Time Scale: Assessing the Impact of ENSO and Volcanic Eruptions. *Journal of Climate*, *24*(9), 2258–2270. https://doi.org/10.1175/2010JCLI3727.1

Guevara-Murua, A., Williams, C. A., Hendy, E. J., Rust, A. C., and Cashman, K. V. (2014). Observations of a stratospheric aerosol veil from a tropical volcanic eruption in December 1808: Is this the "Unknown" ~1809 eruption? *Climate of the Past Discussions*, *10*(2), 1901–1932. https://doi.org/10.5194/cpd-10-1901-2014

Guilderson, T.P., and Schrag, D.P. (1999). Reliability of coral isotope records from the western Pacific warm pool: A comparison using age-optimized records. Paleoceanography, 14(4). doi: 10.1029/1999PA900024

Guillet, S., Corona, C., Stoffel, M., Khodri, M., Lavigne, F., Ortega, P., Eckert, N., Sielenou, P. D., Daux, V., Churakova (Sidorova), O. V., Davi, N., Edouard, J.-L.,

Zhang, Y., Luckman, B. H., Myglan, V. S., Guiot, J., Beniston, M., Masson-Delmotte, V., and Oppenheimer, C. (2017). Climate response to the Samalas volcanic eruption in 1257 revealed by proxy records. *Nature Geoscience*, *10*(2), 123–128. https://doi.org/10.1038/ngeo2875

Hastenrath, Stefan. (1991) Climate Dynamics of the Tropics. Springer Netherlands, 8(1), doi:10.1007/978-94-011-3156-8

Heiss, G.A. (1994). Coral reefs in the Red Sea: Growth, production and stable isotopes. GEOMAR Report, 32:1-141.

Hennekam, R., Zinke, J., van Sebille, E., ten Have, M., Brummer, G.-J.A., and Reichart, G.-J. (2018). Cocos (Keeling) corals reveal 200 years of multi-decadal modulation of southeast Indian Ocean hydrology by Indonesian Throughflow. Paleoceanography and Paleoclimatology, 33. doi: 10.1002/2017PA003181

Hereid, Kelly A., Quinn, Terrence M., Taylor, Frederick W., Shen, Chuan-Chou., Edwards, R. Lawrence., and Cheng, Hai. (2013). Coral record of reduced El Niño activity in the early 15th to middle 17th centuries. Geology, 41(1), 51-54. doi: 10.1130/G33510.1

Hetzinger, S., M. Pfeiffer, W.-C. Dullo, D. Garbe-Schönberg, and J. Halfar. (2010). Rapid 20th century warming in the Caribbean and impact of remote forcing on climate in the northern tropical Atlantic as recorded in a Guadeloupe coral. Palaeogeography, Palaeoclimatology, Palaeoecology, 296(1-2), 111-124. http://dx.doi.org/10.1016/j.palaeo.2010.06.019

Hetzinger, S., M. Pfeiffer, W.-C. Dullo, N. Keenlyside, M. Latif, and J. Zinke. (2008). Caribbean coral tracks Atlantic Multidecadal Oscillation and past hurricane

activity. Geology, 36, 11-14. doi:10.1130/G24321A.1

Huang, H., Winter, J. M., Osterberg, E. C., Horton, R. M., and Beckage, B. (2017). Total and extreme precipitation changes over the Northeastern United States. *18*(6), 1783–1798. https://doi.org/10.1175/JHM-D-16-0195.1.

Iles, C. E., and Hegerl, G. C. (2014). The global precipitation response to volcanic eruptions in the CMIP5 models. *Environmental Research Letters*, *9*(10), 104012. https://doi.org/10.1088/1748-9326/9/10/104012

Iles, C. E., Hegerl, G. C., Schurer, A. P., and Zhang, X. (2013). The effect of volcanic eruptions on global precipitation: Volcanoes and Precipitation. *Journal of Geophysical Research: Atmospheres*, *118*(16), 8770–8786. https://doi.org/10.1002/jgrd.50678

Inoue, Mayuri., Suzuki, Atsushi., Masato, Nohara., Kohei, Hibino., and Hodaka, Kawahata. (2007). Empirical assessment of coral Sr/Ca and Mg/Ca ratios as climate proxies using colonies grown at different temperatures. Geophysical Research Letters, 34(L12611). doi:10.1029/2007gl029628.

Izumo, T., Khodri, M., Lengaigne, M., and Suresh, I. (2018). A Subsurface Indian Ocean Dipole Response to Tropical Volcanic Eruptions. *Geophysical Research Letters*, *45*(17), 9150–9159. https://doi.org/10.1029/2018GL078515

Jimenez, Gloria., Cole, Julia E., Thompson, Diane M., and Tudhope, Alexander W. (2018). Northern Galápagos corals reveal twentieth century warming in the eastern tropical Pacific. Geophysical Research Letters, 45. doi: 10.1002/2017GL075323

Jones, P. D., Briffa, K. R., Osborn, T. J., Lough, J. M., van Ommen, T. D., Vinther, B. M., Luterbacher, J.,Wahl, E. R., Zwiers, F. W., Mann, M. E., Schmidt, G. A.,

Ammann, C. M., Buckley, B. M., Cobb, K. M., Esper, J., Goosse, H., Graham, N., Jansen, E., Kiefer, T., and Xoplaki, E. (2009). High-resolution palaeoclimatology of the last millennium: A review of current status and future prospects. *The Holocene*, *19*(1), 3–49. https://doi.org/10.1177/0959683608098952

Joseph, R., and Zeng, N. (2011). Seasonally Modulated Tropical Drought Induced by Volcanic Aerosol. *Journal of Climate*, *24*(8), 2045–2060. https://doi.org/10.1175/2009JCLI3170.1

Kessler, W. S., and McPhaden, M. J. (1995). The 1991–1993 El Niño in the central Pacific. Deep Sea Research Part II: Topical Studies in Oceanography, 42(2–3), 295–333. https://doi.org/10.1016/0967-0645(95)00041-N

Kilbourne, K. H., Quinn, T. M., Taylor, F. W., Delcroix, T., and Gouriou, Y. (2004). El Niño-Southern Oscillation-related salinity variations recorded in the skeletal geochemistry of a *Porites* coral from Espiritu Santo, Vanuatu: Coral Record of Salinity Variations. *Paleoceanography*, *19*(4), https://doi.org/10.1029/2004PA001033

Kilbourne, K.H., Quinn, T.M., Webb, R., Guilderson, T., Nyberg, J., and Winter, A. (2008). Paleoclimate proxy perspective on Caribbean climate since the year 1751: Evidence of cooler temperatures and multidecadal variability. Paleoceanography, 23(PA3220)

Kuhnert, H., Crüger, T., and Pätzold, J. (2005). NAO signature in a Bermuda coral Sr/Ca record. Geochemistry, Geophysics, Geosystems, 6(4). doi: 10.1029/2004GC000786

Kuhnert, H., Pätzold, J., Hatcher, B., Wyrwoll, K.-H., Eisenhauer, A., Collins, L.B.,

Zhu, Z.R., and Wefer, G. (1999). A 200-year coral stable oxygen isotope record from a high-latitude reef off Western Australia. Coral Reefs, 18, 1-12. doi: 10.1007/s003380050147

Kuhnert, H., Pätzold, J., Wyrwoll, K., and Wefer, G. (2000). Monitoring climate variability over the past 116 years in coral oxygen isotopes from Ningaloo Reef, Western Australia. International Journal of Earth Sciences, 88, 725-732. doi: 10.1007/s005310050300

Lacis, A., Hansen, J., and Sato, M. (1992). Climate Forcing by Stratospheric Aerosols. 19(15),1607–1610, https://doi.org/10.1029/92GL01620

Lechleitner, F. A., Breitenbach, S. F. M., Rehfeld, K., Ridley, H. E., Asmerom, Y., Prufer, K. M., Marwan, N., Goswami, B., Kennett, D. J., Aquino, V. V., Polyak, V., Haug, G. H., Eglinton, T. I., and Baldini, J. U. L. (2017). Tropical rainfall over the last two millennia: Evidence for a low-latitude hydrologic seesaw. *Scientific Reports*, *7*(1), 45809. https://doi.org/10.1038/srep45809

LeGrande, A. N., Tsigaridis, K., and Bauer, S. E. (2016). Role of atmospheric chemistry in the climate impacts of stratospheric volcanic injections. *Nature Geoscience*, *9*(9), 652–655. https://doi.org/10.1038/ngeo2771

Lehner, F., Schurer, A. P., Hegerl, G. C., Deser, C., and Frölicher, T. L. (2016). The importance of ENSO phase during volcanic eruptions for detection and attribution. *Geophysical Research Letters*, *43*(6), 2851–2858. https://doi.org/10.1002/2016GL067935

Linsley, B.K., Dunbar, R.B., Wellington, G.M., and Mucciarone, D.A. (1994). A coral-based reconstruction of Intertropical Convergence Zone variability over Central

America since 1707. Journal of Geophysical Research 99(C5), 9977-9994.

Linsley, B.K., Kaplan, A., Gouriou, Y., Salinger, J., deMenocal, P.B., Wellington, G.M., and Howe, S.S. (2006). Tracking the extent of the South Pacific Convergence Zone since the early 1600s. Geochemistry, Geophysics, Geosystems, 7(Q05003). doi: 10.1029/2005GC001115

Linsley, B.K., Ren, L., Dunbar, R.B., and Howe, S.S. (2000). El Niño Southern Oscillation (ENSO) and decadal-scale climate variability at 10N in the eastern Pacific from 1893 to 1994: A coral-based reconstruction of from Clipperton Atoll. Paleoceanography 15(3):322-335.

Man, W., Zhou, T., and Jungclaus, J. H. (2014). Effects of Large Volcanic Eruptions on Global Summer Climate and East Asian Monsoon Changes during the Last Millennium: Analysis of MPI-ESM Simulations. *Journal of Climate*, *27*(19), 7394–7409. https://doi.org/10.1175/JCLI-D-13-00739.1

Mann, G., Dhomse, S., Deshler, T., Timmreck, C., Schmidt, A., Neely, R., and Thomason, L. (2015). Evolving particle size is the key to improved volcanic forcings. *23*(2), doi: 10.22498/pages.23.2.52

Mann, M. E., Fuentes, J. D., and Rutherford, S. (2012). Underestimation of volcanic cooling in tree-ring-based reconstructions of hemispheric temperatures. *Nature Geoscience*, *5*(3), 202–205. https://doi.org/10.1038/ngeo1394

Mann, Michael E., Zhang, Zhihua., Hughes, Malcolm K., Bradley, Raymond S., Miller, Sonya K., Rutherford, Scott., Ni, Fenbiao. (2008). Proxy-based reconstructions of hemispheric and global surface temperature variations over the past two millennia. PNAS, 105 (36),13252–13257. doi10.1073pnas.0805721105.

Marshall, L., Schmidt, A., Toohey, M., Carslaw, K. S., Mann, G. W., Sigl, M., Khodri, M., Timmreck, C., Zanchettin, D., Ball, W. T., Bekki, S., Brooke, J. S. A., Dhomse, S., Johnson, C., Lamarque, J.-F., LeGrande, A. N., Mills, M. J., Niemeier, U., Pope, J. O., and Tummon, F. (2018). Multi-model comparison of the volcanic sulfate deposition from the 1815 eruption of Mt. Tambora. *Atmospheric Chemistry and Physics*, *18*(3), 2307–2328. https://doi.org/10.5194/acp-18-2307-2018

McCormick, M. P., and Veiga, R. E. (1992). SAGE II measurements of early Pinatubo aerosols. *19*(2), 155–158. https://doi.org/10.1029/91GL02790

McCulloch, M. T., Gagan, M. K., Mortimer, G. E., Chivas, A. R., and Isdale, P. J. (1994). A high-resolution Sr/Ca and $\delta^{18}O$ coral record from the Great Barrier Reef, Australia, and the 1982-1983 El Niño. *58*(12), 2747-2754. https://doi.org/OOM-7037(94)00058-l

McGraw, M. C., Barnes, E. A., and Deser, C. (2016). Reconciling the observed and modeled Southern Hemisphere circulation response to volcanic eruptions. *Geophysical Research Letters*, *43*(13), 7259–7266. https://doi.org/10.1002/2016GL069835

McGregor, Shayne, and Timmermann, A. (2011). The Effect of Explosive Tropical Volcanism on ENSO. *Journal of Climate*, *24*(8), 2178–2191. https://doi.org/10.1175/2010JCLI3990.1

McPhaden, M. J., Zebiak, S. E., and Glantz, M. H. (2006). ENSO as an Integrating Concept in Earth Science. *Science*, *314*(5806), 1740–1745. https://doi.org/10.1126/science.1132588

Mignot, J., Khodri, M., Frankignoul, C., and Servonnat, J. (2011). Volcanic impact on

the Atlantic Ocean over the last millennium. Climate of the Past Discussions, European Geosciences Union, 7, 2511-2554. <10.5194/CPD-7-2511-2011>. <hal-00755362>

Moustafa, Yaser Ahmed., Pätzold, Jürgen., Loya, Yossi., Wefer, Gerold (2000): Stable isotope records of corals from the northern Red Sea. PANGAEA, https://doi.org/10.1594/PANGAEA.712061,

Nakamura, N., H. Kayanne, H. Iijima, T.R. McClanahan, S.K. Behera, and T. Yamagata. (2009). Mode shift in the Indian Ocean climate under global warming. Geophys. Res. Lett., 36(L23708), doi:10.1029/2009GL040590.

Neelin, J. D., Battisti, D. S., Hirst, A. C., Jin, F.-F., Wakata, Y., Yamagata, T., and Zebiak, S. E. (1998). ENSO theory. *Journal of Geophysical Research: Oceans*, *103*(C7), 14261–14290. https://doi.org/10.1029/97JC03424

Neukom, R., Schurer, A. P., Steiger, Nathan. J., and Hegerl, G. C. (2018). Possible causes of data model discrepancy in the temperature history of the last Millennium. *Scientific Reports*, *8*(1), 7572. https://doi.org/10.1038/s41598-018-25862-2

Newman, M., Alexander, M. A., Ault, T. R., Cobb, K. M., Deser, C., Di Lorenzo, E., Mantua, N. J., Miller, A. J., Minobe, S., Nakamura, H., Schneider, N., Vimont, D. J., Phillips, A. S., Scott, J. D., and Smith, C. A. (2016). The Pacific Decadal Oscillation, Revisited. *Journal of Climate*, *29*(12), 4399–4427. https://doi.org/10.1175/JCLI-D-15-0508.1

Nurhati, I. S., Cobb, K. M., and Di Lorenzo, E. (2011). Decadal-Scale SST and Salinity Variations in the Central Tropical Pacific: Signatures of Natural and Anthropogenic Climate Change. *Journal of Climate*, *24*(13), 3294–3308.

https://doi.org/10.1175/2011JCLI3852.1

Nurhati, I.S., Cobb, K.M., Charles, C.D., and Dunbar, R.B. (2009). Late 20th century warming and freshening in the central tropical Pacific. Geophys. Res. Lett., 36(L21606), doi:10.1029/2009GL040270

Osborne, Michael C., Dunbar, Robert B., Mucciarone, David A., Druffel, Ellen., and Sanchez-Cabeza, Joan-Albert. (2014). A 215-yr coral $d^{18}O$ time series from Palau records dynamics of the West Pacific Warm Pool following the end of the Little Ice Age. Coral Reefs. doi: 10.1007/s00338-014-1146-1

Otto-Bliesner, B. L., Brady, E. C., Fasullo, J., Jahn, A., Landrum, L., Stevenson, S., Rosenbloom, N., Mai, A., and Strand, G. (2016). Climate Variability and Change since 850 CE: An Ensemble Approach with the Community Earth System Model. *Bulletin of the American Meteorological Society*, *97*(5), 735–754. https://doi.org/10.1175/BAMS-D-14-00233.1

PAGES Hydro2k Consortium, Smerdon, J.E.; Luterbacher, J; Phipps, S.J.; Anchukaitis, K.J.; Ault, T.; Coats, S.; Cobb, K.M.; Cook, B.I.; Colose, C.; Felis, T.;Gallant, A.; Jungclaus, J.H.; Konecky, B.; LeGrande, A.; Lewis, S.; Lopatka, A.S.; Man, W.; Mankin, J J.S.; Maxwell, T. Otto-Bliesner, B.L.; Partin, J.W. ; Singh, D.; Steiger, N.J.; Stevenson, S.; Tierney, J.E.; Zanchettin, D.; Zhang, H.; Atwood, A.R; Andreu-Hayles, L.; Baek, S.H.; Buckley, B.; Cook, E.R.; D'Arrigo, R.; Dee, S.G.; Griffiths, M.; Kulkarni, C.; Kushnir, Y.; Lehner, F.; Leland, C.; Linderholm, H.W.; Okazaki, A.; Palmer, J.; Piovano, E.; Raible, C.C.; Rao, M.P.; Scheff, J.; Schmidt, G.A.; Seager, R.; Widmann, M.; Williams, A.P.; Xoplaki, E. (2017). Comparing proxy and model estimates of hydroclimate variability and change over the

Common Era. *Clim. Past*, **13**, 1851-1900, doi:10.5194/cp-13-1851-2017.

PAGES2k Consortium (2017a). A global multiproxy database for temperature reconstructions of the Common Era. Scientific Data, 4(1), 170088. https://doi.org/10.1038/sdata.2017.88

Paik, S., and Min, S.-K. (2018). Assessing the Impact of Volcanic Eruptions on Climate Extremes Using CMIP5 Models. *Journal of Climate*, *31*(14), 5333–5349. https://doi.org/10.1175/JCLI-D-17-0651.1

Parker, D. E. (1996). The Impact of Mount Pinatubo on World-Wide Temperatures. 12. Research Gate. https://10.1002/(SICI)1097-0088(199605)16:53.0.CO;2-J

Pausata, F. S. R., Chafik, L., Caballero, R., and Battisti, D. S. (2015). Impacts of high-latitude volcanic eruptions on ENSO and AMOC. *Proceedings of the National Academy of Sciences*, *112*(45), 13784–13788. https://doi.org/10.1073/pnas.1509153112

Pfeiffer, M., Timm, O., Dullo, W.C., Podlech, S. (2004). Oceanic forcing of interannual and multidecadal climate variability in the southwestern Indian Ocean: Evidence from a 160 year coral isotopic record (La Reunion, 55E, 21S). Paleoceanography, 19. doi: 10.1029/2003PA000964

Quinn, T.M., Crowley, T.J., and Taylor, F.W. (1996). New stable isotope results from a 173-year coral record from Espiritu Santo, Vanuatu. Geophysical Research Letters, 23.

Quinn, T.M., Taylor, F.W., and Crowley, T.J. (2006). Coral-based climate variability in the Western Pacific Warm Pool since 1867. Journal of Geophysical Research: Oceans, 111. doi: 10.1029/2005JC003243

Raible, C. C., Brönnimann, S., Auchmann, R., Brohan, P., Frölicher, T. L., Graf, H.-F., Jones, P., Luterbacher, J., Muthers, S., Neukom, R., Robock, A., Self, S., Sudrajat, A., Timmreck, C., and Wegmann, M. (2016). Earth system effects: Tambora 1815 as a test case for high impact volcanic eruptions. *Wiley Interdisciplinary Reviews: Climate Change*, *7*(4), 569–589. https://doi.org/10.1002/wcc.407

Ramos, R.D., Goodkin, N.F., Siringan, F.P., and Hughen, K.A. (2017). Diploastrea heliopora Sr/Ca and d18O records from northeast Luzon, Philippines: an assessment of inter-species coral proxy calibrations and climate controls of sea surface temperature and salinity. Paleoceanography, 32(4), 424-438. doi: 10.1002/2017PA003098

Ren, L., Linsley, B. K., Wellington, G. M., Schrag, D. P., and Hoegh-Guldberg, O. (2002). Deconvolving the $d^{18}O$ seawater component from subseasonal coral $d^{18}O$ and Sr/Ca at Rarotonga in the southwestern subtropical Pacific for the period 1726 to *1997. 67(9):1609–1621.doi:10.1016/S0016-7037(02)00917-1*

Robock, A. (2000). Volcanic eruptions and climate. *Reviews of Geophysics*, *38*(2), 191–219. https://doi.org/10.1029/1998RG000054

Robock, A. (2014). Stratospheric aerosol geoengineering. 183–197. https://doi.org/10.1063/1.491618.

Robock, Alan and Jianping Mao, (1995). The volcanic signal in surface temperature observations. J. Climate, 8, 1086-1103.

Saha, N., Rodriguez-Ramirez, A., Nguyen, A.D., Clark, T.R., Zhao, J.X., and Webb, G.E. (2017). Seasonal to decadal scale influence of environmental drivers on Ba/Ca and Y/Ca in coral aragonite from the southern Great Barrier Reef.

Paleoceanography, submitted.

Schmidt, G. A. (2010). Enhancing the relevance of palaeoclimate model/data comparisons for assessments of future climate change *Journal of Quaternary Science*, *25*(1), 79–87. https://doi.org/10.1002/jqs.1314

Shindell, D. T., Schmidt, G. A., Mann, M. E., Rind, D., and Waple, A. (2001). Solar Forcing of Regional Climate Change During the Maunder Minimum. *Science*, *294*(5549), 2149–2152. https://doi.org/10.1126/science.1064363

Sigl, M., Winstrup, M., McConnell, J. R., Welten, K. C., Plunkett, G., Ludlow, F., Büntgen, U., Caffee, M., Chellman, N., Dahl-Jensen, D., Fischer, H., Kipfstuhl, S., Kostick, C., Maselli, O. J., Mekhaldi, F., Mulvaney, R., Muscheler, R., Pasteris, D. R., Pilcher, J. R., and Woodruff, T. E. (2015). Timing and climate forcing of volcanic eruptions for the past 2,500 years. *Nature*, *523*(7562), 543–549. https://doi.org/10.1038/nature14565

Sivaguru, M., Fouke, KW., Todorov, L., Kingsford, MJ., Fouke, KE., Trop, JM., and Fouke, BW (2019) Correction Factors for δ18O-Derived Global Sea Surface Temperature Reconstructions from Diagenetically Altered Intervals of Coral Skeletal Density Banding. Front. Mar. Sci. 6(306). doi: 10.3389/fmars.2019.00306.

Smith, D. M., Booth, B. B. B., Dunstone, N. J., Eade, R., Hermanson, L., Jones, G. S., Scaife, A. A., Sheen, L., and Thompson, V. (2016). Role of volcanic and anthropogenic aerosols in the recent global surface warming slowdown. *Nature Climate Change*, *6*(10), 936–940. https://doi.org/10.1038/nclimate3058

Sowa, Kohki., Watanabe, Tsuyoshi., Nakamura, Takashi., Sakai, Saburo., Sakamoto, Tatsuhiko. (2013). Estimation of uncertainty for massive Porites coral skeletal

density. JAMSTEC Rep. Res. Dev., 16, 31-39.

Stenchikov, G., Delworth, T. L., Ramaswamy, V., Stouffer, R. J., Wittenberg, A., and Zeng, F. (2009). Volcanic signals in oceans. *Journal of Geophysical Research*, *114*(D16), D16104. https://doi.org/10.1029/2008JD011673

Stevenson, S., Fasullo, J. T., Otto-Bliesner, B. L., Tomas, R. A., and Gao, C. (2017). Role of eruption season in reconciling model and proxy responses to tropical volcanism. *Proceedings of the National Academy of Sciences*, *114*(8), 1822–1826. https://doi.org/10.1073/pnas.1612505114

Stevenson, S., Otto-Bliesner, B., Fasullo, J., and Brady, E. (2016). "El Niño Like" Hydroclimate Responses to Last Millennium Volcanic Eruptions. *Journal of Climate*, *29*(8), 2907–2921. https://doi.org/10.1175/JCLI-D-15-0239.1

Sun, Y., M. Sun, G. Wei, T. Lee, B. Nie, and Z. Yu. 2004. Strontium contents of a Porites coral from Xisha Island, South China Sea: a proxy for sea-surface temperature of the 20th century. Paleoceanography 19:PA2004.

Swart, P.K., G.F. Healy, R.E. Dodge, P. Kramer, H.J. Hudson, R.B. Halley, and M.B. Robblee. (1996). The stable oxygen and carbon isotopic record from a coral growing in Florida Bay: A 160 year record of climatic and anthropogenic influence. Palaeogeography, Palaeoclimatology, Palaeoecology 123(1-4), 219-237.

Swart, P.K., R.E. Dodge, and H.J. Hudson. (1996). A 240-year stable oxygen and carbon isotopic record in a coral from South Florida: Implications for the prediction of precipitation in southern Florida. Palaios 11(4):362-375.

Takada, Noriyuki., Suzuki, Atsushi., Ishii, Hiroshi., Hironaka, Katsuyuki., Hironiwa, Takayuki. (2017). Thermoluminescence of coral skeletons: a high-sensitivity proxy

of diagenetic alteration of aragonite. Scientific Reports. 7:17969. doi:10.1038/s41598-017-18269-y

Thordarson, T., and Self, S. (2003). Atmospheric and environmental effects of the 1783–1784 Laki eruption: A review and reassessment. *Journal of Geophysical Research*, *108*(D1), 4011. https://doi.org/10.1029/2001JD002042

Tierney, J. E., N. J. Abram, K. J. Anchukaitis, M. N. Evans, C. Giry, K. H. Kilbourne, C. P. Saenger, H. C. Wu, and J. Zinke (2015), Tropical sea surface temperatures for the past four centuries reconstructed from coral archives, Paleoceanography, 30, 226–252, doi:10.1002/2014PA002717.

Timmreck, C. (2012). Modeling the climatic effects of large explosive volcanic eruptions: Climatic effects of large explosive volcanic eruptions. *Wiley Interdisciplinary Reviews: Climate Change*, *3*(6), 545–564. https://doi.org/10.1002/wcc.192

Tudhope, A., C., Chilcott, Mc Culloch, M., Cook, E., Chappell, J., R., Ellam, Lea, D., Lough, J., Shimmield, G. (2001). Variability in the El Niño Southern Oscillation through a glacial-interglacial cycle. Science, 291, 1511-1517. doi: 10.1126/science.1057969

Tudhope, A., C., Chilcott., Mc Culloch, M., Cook, E., Chappell, J., R., Ellam., Lea, D., Lough, J., Shimmield, G. (2001). Variability in the El Niño Southern Oscillation through a glacial-interglacial cycle. Science, 291, 1511-1517. doi: 10.1126/science.1057969

Tudhope, A.W., Shimmield, G.B., Chilcott, C.P., Jebb, M., Fallick, A.E., and Dalgleish, A.N. (1995). Recent changes in climate in the far western equatorial Pacific and

their relationship to the Southern Oscillation; oxygen isotope records from massive corals, Papua New Guinea. Earth and Planetary Science Letters 136:575-590.

Urban, F.E., Cole, J.E., Overpeck, J.T. (2000). Influence of mean climate change on climate variability from a 155-year tropical Pacific coral record. Nature, 407.

Vargo, L. (2013). Tree-Ring Evidence of North Pacific Volcanically Forced Cooling and Forcing of the Pacific Decadal Oscillation *(PDO)*. 83.

Veettil, B. K., Leandro Bayer Maier, É., Bremer, U. F., and de Souza, S. F. (2014). Combined influence of PDO and ENSO on northern Andean glaciers: A case study on the Cotopaxi ice-covered volcano, Ecuador. *Climate Dynamics*, *43*(12), 3439–3448. https://doi.org/10.1007/s00382-014-2114-8

Wang, J., Yang, B., Ljungqvist, F. C., Luterbacher, J., Osborn, T. J., Briffa, K. R., and Zorita, E. (2017). Internal and external forcing of multidecadal Atlantic climate variability over the past 1,200 years. *Nature Geoscience*, *10*(7), 512–517. https://doi.org/10.1038/ngeo2962

Wang, T., Otterå, O. H., Gao, Y., and Wang, H. (2012). The response of the North Pacific Decadal Variability to strong tropical volcanic eruptions. *Climate Dynamics*, *39*(12), 2917–2936. https://doi.org/10.1007/s00382-012-1373-5

Wegmann, M., Brönnimann, S., Bhend, J., Franke, J., Folini, D., Wild, M., and Luterbacher, J. (2014). Volcanic Influence on European Summer Precipitation through Monsoons: Possible Cause for "Years without Summer"*. *Journal of Climate*, *27*(10), 3683–3691. https://doi.org/10.1175/JCLI-D-13-00524.1

Winter, A., Zanchettin, D., Miller, T., Kushnir, Y., Black, D., Lohmann, G., Burnett, A., Haug, G. H., Estrella-Martínez, J., Breitenbach, S. F. M., Beaufort, L., Rubino, A.,

and Cheng, H. (2015). Persistent drying in the tropics linked to natural forcing. *Nature Communications*, *6*(1), 7627. https://doi.org/10.1038/ncomms8627

Wu, H.C., B.K. Linsley, E.P. Dassié, B. Schiraldi, and P.B. deMenocal. (2013). Oceanographic variability in the South Pacific Convergence Zone region over the last 210 years from multi-site coral Sr/Ca records. Geochem. Geophys. Geosyst., 14, 1435-1453. doi:10.1029/2012GC004293

Wu, H.C., M. Moreau, B.K. Linsley, D.P. Schrag, and T. Corrège. (2014). Investigation of sea surface temperature changes from replicated coral Sr/Ca variations in the eastern equatorial Pacific (Clipperton Atoll). Palaeogeography, Palaeoclimatology, Palaeoecology, 412, 208-222. doi: 10.1016/j.palaeo.2014.07.039

Xu, Y.-Y., Pearson, S., and Halimeda Kilbourne, K. (2015). Assessing coral Sr/Ca–SST calibration techniques using the species Diploria strigosa. *Palaeogeography, Palaeoclimatology, Palaeoecology*, *440*, 353–362. https://doi.org/10.1016/j.palaeo.2015.09.016

Zanchettin, D., Bothe, O., Lehner, F., Ortega, P., Raible, C. C., and Swingedouw, D. (2015). Reconciling reconstructed and simulated features of the winter Pacific/North American pattern in the early 19th century. *Climate of the Past*, *11*(6), 939–958. https://doi.org/10.5194/cp-11-939-2015

Zanchettin, Davide, Bothe, O., Graf, H. F., Lorenz, S. J., Luterbacher, J., Timmreck, C., and Jungclaus, J. H. (2013). Background conditions influence the decadal climate response to strong volcanic eruptions: Volcanic Forcing and Background Climate. *Journal of Geophysical Research: Atmospheres*, *118*(10), 4090–4106. https://doi.org/10.1002/jgrd.50229

Zanchettin, Davide, Khodri, M., Timmreck, C., Toohey, M., Schmidt, A., Gerber, E. P., Hegerl, G., Robock, A., Pausata, F. S. R., Ball, W. T., Bauer, S. E., Bekki, S., Dhomse, S. S., LeGrande, A. N., Mann, G. W., Marshall, L., Mills, M., Marchand, M., Niemeier, U., and Tummon, F. (2016). The Model Intercomparison Project on the climatic response to Volcanic forcing (VolMIP): Experimental design and forcing input data for CMIP6. *Geoscientific Model Development*, *9*(8), 2701–2719. https://doi.org/10.5194/gmd-9-2701-2016

Zebiak, S. E., & Cane, M. A. (1987). *A Model El Niño Southern Oscillation*. *115*.

Zhou, T., Turner, A. G., Kinter, J. L., Wang, B., Qian, Y., Chen, X., Wu, B., Wang, B., Liu, B., Zou, L., and He, B. (2016). GMMIP (v1.0) contribution to CMIP6: Global Monsoons Model Inter-comparison Project. *Geoscientific Model Development*, *9*(10), 3589–3604. https://doi.org/10.5194/gmd-9-3589-2016

Zinke, J., A. Hoell, J.M. Lough, M. Feng, A.J. Kuret, H. Clarke, V. Ricca, K. Rankenburg, and M.T. McCulloch. 2015. Coral record of southeastern Indian Ocean marine heatwaves with intensified Western Pacific temperature gradient. Nature Communications, 6, 8562. doi: 10.1038/ncomms9562

Zinke, J., A. Rountrey, M. Feng, S.P. Xie, D. Dissard, K. Rankenburg, J. Lough, and M.T. McCulloch. 2014. Corals record long-term Leeuwin Current variability including Ningaloo Niño/Niña since 1795. Nature Communications, 5, 3607. doi: 10.1038/ncomms4607

Zinke, J., B. Loveday, C. Reason, W.-C. Dullo, and D. Kroon. (2014). Madagascar corals track sea surface temperature variability in the Agulhas Current core region over the past 334 years. Scientific Reports, 4, 4393. doi: 10.1038/srep04393

Zinke, J., Dullo, W.C., Heiss, G.A., Eisenhauer, A. (2004). ENSO and Indian Ocean subtropical dipole variability is recorded in a coral record off southwest Madagascar for the period 1659 to 1995. Earth and Planetary Science Letters, 228(-1). doi: 10.1016/j.epsl.2004.09.028

Zinke, J., M. Pfeiffer, O. Timm, W.-C. Dullo, D. Kroon, and B. A. Thomassin. (2008). Mayotte coral reveals hydrological changes in the western Indian Ocean between 1881 and 1994. Geophys. Res. Lett., 35, L23707, doi:10.1029/2008GL035634.

Zinke, Jens., Reuning, Lars., Pfeiffer, Miriam., Wassenburg, Jasper A., Hardman, Emily., Jhangeer-Khan, Reshad., Davies, Gareth R., Ng, Curtise K.C., and Kroon, Dick. (2016). A sea surface temperature reconstruction for the southern Indian Ocean trade wind belt from corals in Rodrigues Island (19S, 63E). Biogeosciences, 13, 5827-5847. doi: 10.5194/bg-13-5827-2016